Subsection 2.5.5 Table of Contents

Subsection 2.5.5 List of Tables

Subsection 2.5.5 List of Figures

List of Figures (Continued)

VCS COL 2.0-30-A

2.5.5 Stability of Slopes

This subsection is prepared in accordance with the applicable sections of RG 1.206 (Reference 2.5.5-201).

The information presented in this subsection is based on the results of the site-specific subsurface investigation performed at the VCS site, which is described in Subsection 2.5.4. Note that the detailed data collected from this site-specific subsurface investigation is contained in Appendices 2.5.4-A (power block) and 2.5.4-B (cooling basin/Guadalupe-Blanco River Authority [GBRA] storage water reservoir), included with that subsection.

As described in Subsection 2.5.4.2.1.1, the natural ground surface at and around the power block (refer to Figure 2.5.4-201) at the time of this subsurface investigation was generally level, ranging from approximately elevation 78 feet North American Vertical Datum of 1988 (NAVD 88) to elevation 81 feet (NAVD 88) with an average elevation of 80 feet (NAVD 88). During construction, the power block finish grade elevation is raised approximately 15 feet to elevation 95 feet (NAVD 88).

Given the natural topography and the project earthwork/site grading, there are no safety-related slopes, neither natural nor man-made, which are pertinent to the development of the power block at the VCS site.

Also as described in Subsection 2.5.4.2.1.1, the natural ground surface at the nonsafety-related cooling basin/GBRA storage water reservoir (refer to Figure 2.5.4-202) at the time of this subsurface investigation was gently sloping downward from northwest to southeast, ranging from approximately elevation 80 feet (NAVD 88) to elevation 42 feet (NAVD 88), with an average elevation of 70 feet (NAVD 88). The base level of the cooling basin/GBRA storage water reservoir is elevation 69 feet (NAVD 88). An embankment dam having crest at elevation 102 feet (NAVD 88) surrounds the cooling basin/GBRA storage water reservoir and divides the cooling basin from the adjoining GBRA storage water reservoir. The cooling basin also has interior dikes with crest at elevation 99 feet (NAVD 88).

The details of a preliminary design for the nonsafety-related cooling basin/GBRA storage water reservoir embankment dams are described in this subsection.

2.5.5.1 Slope Characteristics

Figure 2.5.4-213 is a plan view of the cooling basin/GBRA storage water reservoir and its vicinity. To the east, beyond the outside perimeter embankment dam (i.e., east of the GBRA storage water reservoir) there is a more rapid change in topography as the terrain drops to the Guadalupe River Plateau at about elevation 15 feet (NAVD 88). The figure shows the locations of several drainage swales in the area of the easternmost embankment dam, areas where the embankment dam is at its highest (about 60 feet high).

2.5.5.1.1 Description of Subsurface Materials

The subsurface materials below the cooling basin/GBRA storage water reservoir consist of interlayered strata of sands, clayey sands, and clays belonging to the Beaumont Formation. Based on laboratory classification tests and on the information from borings and cone penetration tests, subsurface materials to approximately 600 feet below ground surface are divided into 20 different strata. Details about the properties of each stratum are presented in Subsection 2.5.4.2.1. A description of the properties of subsurface materials deeper than 600 feet below ground surface is also presented in Subsection 2.5.4.2.1.

2.5.5.1.2 Detailed Description of Slopes and Related Features

As noted above, the area occupied by the cooling basin/GBRA storage water reservoir is relatively flat, gently sloping down from northwest to southeast.

Cooling basin/GBRA storage water reservoir embankment dam slopes are typically 4 horizontal:1 vertical (4H:1V) inboard (i.e., interior to the basin/reservoir) and 3H:1V outboard (i.e., exterior to the basin/reservoir), except at the east embankment dam of the GBRA storage water reservoir, where both the inboard and outboard slopes are 3H:1V. Interior dikes have 3H:1V slopes, on both sides. The embankment dams (and the interior dikes) are constructed of compacted earth fill, with fill materials obtained from onsite excavation. Inboard embankment dam slopes (and interior dike slopes) are covered by a soil-cement layer or other suitable material selected at detailed design to protect against erosion. Outboard embankment slopes are topsoiled and seeded.

2.5.5.1.3 Plan View of Excavations, Embankment Fills, and Slopes

The extent of excavation and filling for embankments and interior dikes are shown in plan on Figure 2.5.4-280 and in profile on Figure 2.5.4-281 through 2.5.4-285.

Figures 2.5.5-201 through 2.5.5-208 are horizontal cross sections (at elevation 69 feet, 67 feet, 65 feet, 63 feet, 60 feet, 55 feet, 50 feet, and 45 feet (NAVD 88)) that illustrate subsurface stratigraphy at and below the cooling basin/GBRA storage water reservoir base level. These cross sections show the plan extent of Strata Clay 1 (Top), Clay 1 (Bottom), Clay 3, Sand 1, and Sand 2 within the footprint of the basin/reservoir at each of the respective elevations. The cross sections also show in crosshatching those subareas of the basin/reservoir having ground surface elevation below the corresponding cross section elevation. Figure 2.5.5-201, which illustrates the horizontal cross section at elevation 69 feet (NAVD 88) (i.e., the basin/reservoir base/excavation level), for example, shows that about one-half of the basin/reservoir footprint area is above original ground surface and requires excavation that exposes Strata Clay 1 (Top) and Sand 1, and about one-half of the basin/reservoir footprint area is below the elevation 69 (NAVD 88) feet base/excavation level. Areas of the basin/reservoir footprint that occur below the referenced elevations decrease with depth, as shown in subsequent horizontal cross sections (i.e., Figures 2.5.5-202 through 2.5.5-208). The area near the east dam of the GBRA storage water reservoir at some locations has original ground surface as low as elevation 42 feet (NAVD 88). These locations correspond to the drainage swales mentioned in Subsection 2.5.5.1.

2.5.5.1.4 Profiles of Slopes and Their Foundation

Developed slopes at and around the cooling basin/GBRA storage water reservoir are only those of the man-made embankment dams and interior dikes constructed.

As included in Subsection 2.5.4, Figure 2.5.4-213 is a plan view of the cooling basin/GBRA storage water reservoir showing the locations of the subsurface profiles presented on Figures 2.5.4-214 through 2.5.5-220. Graphic symbols for profiles are explained on Figure 2.5.4-203. Also shown on these profiles are elevations of embankment crest, maximum pool, bottom of basin/reservoir, and approximate original ground surface

elevations. The figures show the vertical and horizontal distribution of strata described in Subsection 2.5.4.2.1.

Four of the above figures (Figures 2.5.4-214, 2.5.5-216, 2.5.4-217, and 2.5.4-220) are subsurface cross sections along the outermost (perimeter) embankments of the basin/reservoir. Considering the subsurface conditions depicted on these profiles, five locations are selected for slope stability analyses. Subsurface stratification at the selected locations (Figures 2.5.4-281 through 2.5.4-285) is based on information from the nearest boring or cone penetration test (CPT) performed during the subsurface investigation. Also shown on these figures are elevations of embankment crest, maximum pool, bottom of basin/reservoir, and approximate original ground surface elevations.

2.5.5.1.5 Subsurface Investigation/Exploration Program and Geologic Features

Planning of the field exploratory program is described in Subsection 2.5.4.2.2.1 and summarized in Table 2.5.4-202. The field program consists of: borings and standard penetration tests (SPTs) N-value measurements; CPTs; tests pits; groundwater observation wells and groundwater testing (slug tests, borehole permeameter tests, and pump tests); geophysical surveys (suspension P-S velocity logging and seismic CPTs); and the collection and analysis of available regional/oil field sonic well logging data.

Tables 2.5.4-237 and 2.5.4-239 summarize as-built boring information and undisturbed sample details, respectively.

Uncorrected SPT N-values are summarized in Table 2.5.4-206. Energy transfer ratio/hammer energy corrections, average corrected SPT $(N_1)_{60}$-values, and corrected SPT $(N_1)_{60}$-values selected for design, are summarized in Tables 2.5.4-207, 2.5.4-209, and 2.5.4.-211, respectively. Uncorrected SPT N-values and corrected SPT $(N_1)_{60}$-values are shown on Figures 2.5.4-226 and 2.5.4-232, respectively. Figure 2.5.4-329 is an example calculation of the conversion from the SPT N-value to the “clean sand equivalent” SPT-$(N_1)_{60cs}$-value for liquefaction evaluation purposes.

CPT values are summarized in Table 2.5.4-213. Corrected CPT tip resistance (q_t) and normalized CPT tip resistance $(q)_{c1n}$ are shown in Figures 2.5.4-236 and 2.5.4-240, respectively. As-built cone penetration test information is summarized in Table 2.5.4-241. Figure 2.5.4-330 is an example calculation of the conversion from uncorrected CPT tip

resistance (q_c) value to the “clean sand equivalent” $(q)_{c1ncs}$ value for liquefaction evaluation purposes. Figures 2.5.4-251, 2.5.4-260, and 2.5.4-265 show empirical correlations of CPT test results with undrained shear strength (s_u) of cohesive (clay) strata, over-consolidation of cohesive (clay) soil strata, and drained friction angle (Φ’) of cohesionless (sand) soil strata, respectively.

As-built test pit information is summarized in Table 2.5.4-243.

Figures 2.5.4-270 and 2.5.4-274 present measured shear (S) wave velocity values versus elevation, and average/recommended S-wave velocity versus elevation profiles, respectively. Table 2.5.4-253 lists the numerical values of the average/recommended S-wave velocity versus elevation profile.

2.5.5.1.6 Groundwater and Seepage

Subsection 2.5.4.6 describes the history of groundwater fluctuations in the area, site-specific groundwater measurements, and the results of hydraulic conductivity testing (i.e., slug testing, borehole permeameter testing, and pump testing). Groundwater levels measured in the observation wells are presented on Figures 2.5.4-288 through 2.5.4-292. As-built observation well information is shown in Table 2.5.4-247. As-built borehole permeameter test information and as-built pumping test information are presented in Tables 2.5.4-248 and 2.5.4-249, respectively.

As described in Subsection 2.4.12, a complete groundwater model is prepared for the VCS site to evaluate post-construction groundwater levels resulting from the maximum water level in the cooling basin/GBRA storage reservoir. The effect of this contained water is a general rise in groundwater levels site-wide. Overall seepage loss through the cooling basin/GBRA storage water reservoir is estimated from the groundwater model, as described in Subsection 2.4.12. Seepage loss laterally through the cooling basin/GBRA storage water reservoir embankment dams, which is additive to the overall seepage loss from the groundwater model, is estimated using the flow net method in developing this subsection. This latter value is approximately 40 gallons per minute (gpm) (assuming embankment fill average hydraulic conductivity of 5×10^{-6} centimeters per second) to 400 gpm (assuming embankment fill average hydraulic conductivity of 5×10^{-5} centimeters per second) for the cooling basin/GBRA storage water reservoir perimeter.

Initial seepage analyses performed, considering flow through and below the embankment dams, indicate that exit gradients at the outboard toe of the embankment dams approach or exceed critical values. To reduce exit gradients to an acceptable value, it is necessary to excavate a 10-foot deep trench at the toe of the embankment dams backfilled with drainage sand material.

2.5.5.1.7 Subsurface Investigation/Exploration

The site-specific subsurface investigation and laboratory testing were conducted for the cooling basin/GBRA storage water reservoir. Scope, methods, and results are presented in the data report titled *Geotechnical Exploration and Testing, Exelon Texas COL Project, Victoria County, Texas, Cooling Basin,* dated July 18, 2008, which is included as Appendix 2.5.4-B. Refer to Subsection 2.5.4.2 and Subsection 2.5.4.4 for details on tests, methods, results, and evaluations.

2.5.5.1.8 Sampling Methods

Refer to the data report noted above, included as Appendix 2.5.4-B.

2.5.5.1.9 Static and Dynamic Soil Properties of Slopes and Their Foundations

Tables 2.5.4-215 and 2.5.4-217 summarize the laboratory testing program and the general physical and chemical properties of embankment dam foundation materials, respectively. The laboratory testing program was prepared to characterize both the static and dynamic engineering properties of the foundation soils and the proposed embankment fill materials. Test results are summarized in Subsection 2.5.4.2.1 and in the following tables and figures:

- Atterberg limits and plasticity chart (Figures 2.5.4-242 and 2.5.4-244)
- Strength tests (Table 2.5.4-219)
- Drained friction angle of cohesionless (sand) strata (Table 2.5.4-219)
- Moisture-density relationships (Table 2.5.4-245)
- Undrained shear strength of cohesive (clay) strata (Table 2.5.4-221 and Figure 2.5.4-246)
- Consolidation tests (Table 2.5.4-223)
- Preconsolidation pressure of cohesive (clay) strata (Figure 2.5.4-253)
- Consolidation test properties of cohesive (clay) strata (Table 2.5.4-225)

- Over-consolidation ratios and preconsolidation pressures of cohesive (clay) strata (Table 2.5.4-227 and Figure 2.5.4-255)
- High strain elastic moduli (Table 2.5.4-229)
- High strain shear moduli (Table 2.5.4-231)
- Shear modulus degradation curves—numerical values (Table 2.5.4-255)
- Damping curves—numerical values (Table 2.5.4-257)
- Resonant Column Torsional Shear (RCTS) numerical test results, embankment fill/sand; Composite “A” (Table 2.5.4-274)
- RCTS numerical tests results, embankment fill/clay; Composite “B” (Table 2.5.4-275)
- RCTS test results: shear modulus degradation, embankment fill/sand, Composite “A” (Figure 2.5.4-309).
- RCTS test results: damping ratio, embankment fill/sand, Composite “A” (Figure 2.5.4-327)
- RCTS test results: shear modulus degradation, embankment fill/clay, Composite “B” (Figure 2.5.4-310)
- RCTS test results: damping ratio, embankment fill/clay, Composite “B” (Figure 2.5.4-328)

2.5.5.1.9.1 Slopes and Foundation Materials

Stability analyses of man-made slopes (embankment dams) require as input the engineering properties of the embankment fills (designated here as Composite “A” and Composite “B”), and the foundation sands and clays on which they are supported. The selection process in the development of Composite “A” and Composite “B” materials, representative of cooling basin/GBRA storage water reservoir embankment fills, is described in Subsection 2.5.4.5.1. Note that recompacted specimens prepared for strength testing from these composite/combined samples are compacted to 95% of modified Proctor (Reference 2.5.4-217) maximum dry densities at 4% above optimum moisture content.

Properties required for slope stability analyses are: total unit weights and drained and undrained shear strengths.

Derivation of the average total unit weight of each soil stratum listed in Table 2.5.5-201 is addressed in Subsection 2.5.4.2.1.

Figure 2.5.5-209 shows the applicability of different laboratory strength tests to the study of slope stability. Three zones along a potential slip surface are identified. Note that soils in the downwards zone are in compression mode, soils in the central/horizontal zone are in a simple shear mode, and soils in the upwards zone are in extension mode. Applicable laboratory tests are: plane strain compression and triaxial compression tests for the downwards zone, direct simple shear tests for the central/horizontal zone, and plane strain extension or triaxial extension tests for the upwards zone.

Reference 2.5.5-205 shows that estimates of undrained shear strengths measured in triaxial compression tests are almost always unconservative because isotropic consolidation in the tests leads to a water content that is too low (which increases the measured strength), and shearing in triaxial compression ignores anisotropy, which therefore leads to the over-estimation of strength. For this project, estimates of the plane strain compression shear strength parameters are based on the results of direct simple shear tests performed on undisturbed samples of foundation materials and recompacted soil samples representative of embankment fill (i.e., Composite “A” and Composite “B”). In accordance with Reference 2.5.5-213, plane strain extension shear strengths are about equal to direct simple shear test results.

2.5.5.1.9.1.1 Embankment Fills

Effective Friction Angle

Table 4.12 in Appendix 2.5.4-B summarizes the results of 12 direct simple shear tests made on each of the two composite samples. The simple shear effective friction angles (Φ’) considered for the selection of design values correspond to the shear strains listed in the table. Average friction angles corresponding to effective vertical pressures less than 8.3 kips per square foot (ksf) (i.e., the largest soil pressure at the base of the highest embankment) are 28.8° and 29.1° for Composite “A” and Composite “B,” respectively.

Of interest to slope stability studies is the friction angle from plane strain compression tests, or equivalent. Effective stress friction angles of granular materials vary, depending on if they are measured in triaxial compression, direct shear, direct simple shear tests, or under plane strain conditions, the latter being higher by 2° to 7°. Reference 2.5.5-214

concludes that the difference in clayey soils is approximately 1° to 2°, a conclusion that is in agreement with Reference 2.5.5-215.

An effective stress friction angle under plane strain conditions equal to 30° for the two Composite materials is adopted for design.

Undrained Shear Strength

Reliable test methods to define the undrained shear strength of embankment fill materials are: the isotropically-consolidated undrained (CIU) saturated triaxial compression test; and the saturated direct simple shear test.

The results of CIU triaxial compression and direct simple shear tests made on samples of the Composite materials are presented in Volume 3 of Appendix 2.5.4-B. Because the undrained shear strength results obtained from the direct simple shear tests show a greater consistency than the results obtained from the CIU triaxial tests, the undrained shear strengths derived under plane strain compression conditions of the two Composite materials are based on the results of the former tests.

Figure 4-37 in Reference 2.5.5-213 shows the value of undrained simple shear strength ratio as a function of test type. In accordance with the the information contained in that figure, the undrained shear strength obtained from plane strain compression tests should be approximately 1.5 times the undrained shear strength obtained from simple shear tests.

Figure 2.5.5-210 shows both the laboratory-obtained undrained shear strengths from simple shear tests (Line A) and the values adopted for slope stability analyses (Line B).

2.5.5.1.9.1.2 Foundation Clays

Effective Friction Angle

The results of direct simple shear tests made on samples of foundation clays are summarized in Table 4.7 of Appendix 2.5.4-B. Friction angles corresponding to the peak shear strains listed in the table were again extracted from the individual laboratory test data sheets in the same appendix.

A plot of 19 effective friction angle (Φ') values corresponding to the effective vertical pressure at failure conditions in the laboratory tests show effective friction angles (Φ') ranging between 25.3° and 33.7° (mean value equal to 29.5°).

As described in Subsection 2.5.5.1.9.1.1, the effective friction angle of clays under plane strain conditions is expected to be higher than the same angle under simple shear conditions by 1° to 2°. Based on this consideration a conservative effective friction angle equal to 28° for foundation clay materials is adopted for slope stability analyses.

Undrained Shear Strength

As noted above, Table 4.7 of Appendix 2.5.4-B summarizes the results of the direct simple shear tests made on samples of foundation clays recovered from various depths. Figure 2.5.5-211 shows the undrained shear strength values given in the table as they vary with depth. A best-fit line to the test results is also shown on the figure. Because the test data is scattered, and a number of test points remain above the best-fit line (i.e., representing lower strengths), a lower-bound best-fit line of the test results above the initial best-fit line is also shown. To be conservative, the lower-bound best-fit line is adopted as representative of the undrained shear strength of the foundation clays under simple shear conditions.

As described in Subsection 2.5.5.1.9.1.1, the undrained shear strength obtained from plane strain compression tests is about 1.5 times the strength of the clay obtained from simple shear tests.

Figure 2.5.5-212 presents the relationship between in situ effective vertical pressure, the best-fit line to all of the data (Line C), the lower-bound best-fit line (Line A), and 1.5 times the lower-bound best-fit line (Line B). The best-fit line for all of the data (Line C) is adopted as representative of the undrained shear strength of foundation clays for slope stability analyses.

2.5.5.1.9.1.3 Foundation Sands

Table 4.6 of Appendix 2.5.4-B summarizes the results of direct shear tests made on nine samples of foundation sands and silts recovered from various depths. Six of the samples are USCS classification SP-SM or SM materials, with fines contents between 7% and 22%, and three are USCS classification ML materials, with fines contents between 55 and 63%. The mean and standard deviation of the test results yield an effective friction angle (Φ') of 37° plus or minus 2°.

A statistical study of the effective friction angle (Φ') derived from empirical relationships with SPT N-values (583 tests), and with CPT tip resistance (q_c) values (1989 tests) show weighted averages of the effective friction angle (Φ') equal to 37.2° and 40.9°, respectively.The empirical

correlations between friction angle and the field SPT N-value blow and the CPT tip resistance (q_c) are based on calibrations done in the laboratory using triaxial tests to find the effective friction angle (Φ') of clean sands, then relating the corresponding relative densities to correlations between these and SPT and CPT results. Because site foundation sands are not clean, the values obtained from the correlations need to be modified. The laboratory-obtained direct shear test results can also be used to calibrate the correlations from the two field test methods because the direct shear test results reflect the actual fines contents of the sands. When this is done, it can be concluded that the "calibration factor" between the direct shear laboratory test results and the SPT N-value correlation results is approximately 1 because the weighted average friction angle based on the SPT correlation (again, from 583 SPT N-values) is 37.2, a value that is comparable to the average direct shear friction angle (37°). An average "calibration factor" for the CPT correlation, would however, be approximately 90% (e.g., 37°/40.9° x 100%).

Note that neither the direct shear test results, nor the SPT N-value correlation, nor the CPT q_c-value correlation take into account the three-dimensional plane strain loading on the foundation sands.

Several authors (References 2.5.5-216, 2.5.5-217, 2.5.5-218, and 2.5.5-219) have studied the influence of test conditions on effective friction angle (Φ'). Based on the references, the plane strain friction angle of foundation sands should be expected to be 2° to 7° higher than the effective friction angle obtained under triaxial compression conditions (refer also to the description of the effective friction angle of embankment fills in Subsection 2.5.5.1.9.1.1). Because the average effective friction angle measured in direct shear tests (which approximately equals the effective friction angle from triaxial compression tests, in accordance with Reference 2.5.5-216) is 37°, the effective friction angle under plane strain conditions is 37° plus the plane strain increase (2° to 7°), that is, a plane strain effective friction angle in the range of 39° to 44°.

For slope stability analyses a conservative value of effective friction (Φ') equal to 40°, and an effective cohesion (c') equal to 0.4 ksf are recommended for foundation sand materials (Figure 2.5.5-213).

2.5.5.1.9.2 Drainage Materials

Two sand samples collected from a local quarry operation in Victoria, Texas are studied for the construction of embankment dam drains (refer to Subsection 2.5.4.5.1 for additional detail): one sample of material meeting the requirements of ASTM C 33 (Reference 2.5.4-218), fine aggregate for concrete; and a second sample of material meeting the requirements of ASTM C 144 (Reference 2.5.4-219), mortar sand. The 15% diameter (D_{15}) size of the two sands is 0.26 mm. To meet filter criteria, drainage sand materials need to be compatible with the particle size distributions of the four base materials with which they are in contact, namely embankment fill materials (Composite A and Composite B), foundation sand materials (Stratum Sand 1), and foundation clay materials (Stratum Clay 1 [Top]). Filter criteria are described in References 2.5.5-211 and 2.5.5-212.

Filter criteria proposed in Reference 2.5.5-211 are as follows:

- Sands having D_{15} of about 0.5 millimeters (mm) or less are suitable filters even for the finest clays.
- For sandy silts and clays with significant sand content (i.e., D_{85} of 0.1 mm to 0.5 mm) the existing filter criterion $D_{15}/D_{85} \leq 5$ is conservative and reasonable, where:
- D_{15} =Particle size of the filter soil (i.e., the drainage sand), for which 15% by dry weight of particles are smaller, and
- D_{85} =Particle size of the base soil, for which 85% by dry weight of particles are smaller.

Table 2.5.5-203 shows the compatibility of the two drainage sand materials with the above criteria.

Filter criteria proposed in Reference 2.5.5-212 are as follows:

- Select the base soil material that requires the smallest D_{15} size. (e.g., Stratum Clay 1 [Top]).
- Place the base soil in a category based on the percent passing the No. 200 sieve in accordance with Table D-1 of the reference. (e.g., Category 2 for Stratum Clay 1 [Top]).
- Determine the maximum D_{15} for the filter in accordance with Table D-2 of the reference (e.g., for Category 2—D_{15} of the proposed drainage material less than or equal to 0.7mm). D_{15} size of the proposed drain material is 0.26 mm, which satisfies the criteria.

As noted above, the D_{15} size of both drainage sand materials is 0.26 mm (≤0.7mm), which satisfies the above criteria.

Laboratory direct shear tests show a friction angle equal to 37° for the ASTM C 33 (Reference 2.5.4-218) fine aggregate for concrete material, and a friction angle of 36° for the ASTM C 144 (Reference 2.5.4-219) mortar sand material. Total unit weights are 111 and 108 pounds per cubic foot (pcf), respectively. For slope stability analyses, an average friction angle of 36° and an average total unit weight equal to 110 pcf are recommended for drainage sand materials.

2.5.5.1.10 Geotechnical Engineering Parameters Selected for Design

Evaluation of the stability of embankment dam slopes is based on the following parameters:

- Total unit weights (Table 2.5.5-201). Note that for slope stability analyses, a total unit weight of 126 pcf is used for all foundation clays and foundation sands, and a total weight of 134 pcf is used for embankment fill.
- Effective (drained) and total (undrained) shear strengths (Table 2.5.5-202).
- Undrained shear strengths, embankment fill/sand (Composite “A”) and embankment fill/clay (Composite “B”) (Figure 2.5.5-210).
- Undrained shear strengths, Foundation Clay 1 (Top) (Figure 2.5.5-212).

2.5.5.1.11 Weak Zones, Clay Lenses, and Liquefiable Materials

The existing ground surface at the cooling basin/GBRA storage water reservoir is covered with a 1-foot-thick layer of organic soil that is removed prior to the construction of embankments. Shallow investigations (less than 10 feet deep) disclosed the presence of a surficial loose layer of sand along the east dam of the GBRA storage water reservoir (refer also to Subsections 2.5.4.8 and 2.5.4.12). This sand is removed or recompacted prior to construction of the embankment dams. Deeper field investigations, below about 10 feet, did not disclose the presence of weak zones, clay lenses, or liquefiable materials. Subsection 2.5.4.8 documents the results of a detailed liquefaction evaluation of the granular deposits encompassing the whole cooling basin/GBRA storage water reservoir area.

2.5.5.2 Design Criteria and Analyses

2.5.5.2.1 Performance of Earth Dam Slopes; Case Histories

This section reviews case histories compiled through the years on the field performance of slopes similar to those of the cooling basin/GBRA storage water reservoir embankment dams.

2.5.5.2.1.1 Static Performance

Reference 2.5.5-204 compiles a list of 35 earth dam failures occurring between 1879 and 1938. Causes of dam failures are listed as foundation and/or embankment low shear strength, inboard drawdown, overtopping, and piping.

Reference 2.5.5-207 lists the unsatisfactory performance of 206 earth dams between the years 1901 and 1951. The author differentiates the reasons for poor performance into several categories including overtopping, foundation or embankment piping, outboard slope sliding, and inboard slope drawdown.

Reference 2.5.5-210 reviews the data compiled in Reference 2.5.5-207 and concludes that:

- Inboard slope slides caused by drawdown have not often threatened to cause complete failure of the dam because they usually happen when the reservoir has dropped below a dangerous level.
- Embankment or foundation slides during construction never threaten a catastrophic failure unless water is retained while the dam is built. Slope and crest erosion by waves, wind, and rain do not lead to danger of complete failure except in special circumstances.

2.5.5.2.1.2 Seismic Performance

Reference 2.5.5-208 studies the performance of embankments that are subjected to the earthquakes listed below:

- 1906 San Francisco earthquake, 32 earth embankments
- 1923 Kanto earthquake, 3 earth embankments
- 1925 Santa Barbara earthquake, 1 sand embankment
- 1939 Ojika, Japan earthquake, 74 earth embankments
- 1940 El Centro earthquake, several dykes and canals
- 1943 Chile earthquake, dumped rock fill embankment
- 1946 Nankai earthquake, 50 embankments

- 1948 Fukui earthquake, 1 earth embankment
- 1952 Kern County earthquake, 7 earth embankments
- 1954 Fallon, Nevada earthquake, 3 earth embankments
- 1959 Hegben earthquake, 1 earth embankment
- 1961 Kita-Muto earthquake, 1 rock fill embankment
- 1964 Alaska earthquake, 1 earth embankment
- 1968 Tokachi-Oki earthquake, 93 earth embankments
- 1971 San Fernando earthquake, 44 earth embankments

A careful review of the experiences gained from the above case histories lead the investigators to several conclusions, three of which are relevant to the cooling basin/GBRA storage water reservoir embankment dams:

- Virtually any well-built dam can withstand moderate earthquake shaking, for example with peak acceleration levels of about 0.20g or more, with no detrimental effect.
- Dams constructed of clayey soils on clay or rock foundations have withstood strong shaking ranging from 0.35g to 0.80g from a Magnitude 8.25 earthquake with no apparent damage.
- There is ample field evidence that well-built dams can withstand moderate shaking with peak accelerations up to at least 0.20g with no harmful effects.

The Federal Emergency Management Agency (FEMA) in 2005 prepared and published *The Federal Guidelines for Dam Safety* (Reference 2.5.5-203), which documents the good performance of several dams during three earthquakes subsequent to the those included in Reference 2.5.5-208, namely the 1985 Michoacan; 1987 Edgecumbe, New Zealand; and 1994 Northridge earthquakes. This report concludes, “To summarize, experience has shown that well-compacted, impervious rolled-fill dams are resistant to earthquake forces, provided they are constructed on rock or overburden foundations resistant to liquefaction.”

2.5.5.2.2 Adopted Factors of Safety for Slope Stability and Seepage Analyses

This section identifies the stages in the life of an embankment dam and methodologies to analyze stability and lists the criteria adopted for the design and construction of the cooling basin/GBRA storage water reservoir embankment dams.

2.5.5.2.2.1 Current Methods for Static and Dynamic Dam Design Practices

Although the embankment dams at the cooling basin/GBRA storage water reservoir are nonsafety-related from a nuclear safety standpoint, the design criteria and methodologies adopted for their design are nevertheless significant given the importance of the basin/reservoir structure and the environment in which it exists. A review of the selected design criteria and methodologies follows.

In general, there are five stages in the life of an embankment dam for which its stability must be analyzed:

- Case 1: Shortly After Construction. Applicable to both the inboard and outboard slopes.
- Case 2: Steady-State Seepage. Pore water pressures in the outboard slope reach the maximum when the reservoir has been full long enough for seepage water to percolate through the embankment (steady-state condition), at which time the outboard slope factor of safety (FOS) is at its lowest.
- Case 3: Rapid Drawdown. The FOS of the inboard slope of the embankment reaches its minimum value by lowering the inboard water level after the steady-state stage has developed.
- Case 4: Slope deformation during the design seismic event.
- Case 5: Post-earthquake stability of the outboard slope.

2.5.5.2.2.2 Shortly After Construction Case

Although experience shows that slope failures of earth dams at the time of construction have not occurred as frequently as slope failures during the steady-state condition, it is customary to evaluate the stability of slopes under this condition. An analysis using the effective stress shear strength parameters (ϕ', c') requires knowledge of the pore pressures induced by construction. The difficulty encountered in an analysis using the effective stress shear strength parameters is that the prediction of the pore pressures is difficult. The principal factors controlling pore pressure setup are:

- Placement moisture content and density of embankment fill
- State of stress in the zone of the embankment under consideration
- Rate of dissipation of pore pressure and duration of construction

Reference 2.5.5-210, describes the shortcomings of the effective stress analysis approach and concludes, as Reference 2.5.5-218 does, that there is no method to reliably estimate the pore pressures.

For these reasons, References 2.5.5-210, 2.5.5-212, and 2.5.5-218 recommend that for small earth dams built with clay softer than their foundation soils, the stability shortly after construction is estimated based on a total stress (Φ = 0) undrained analysis rather than on an effective stress analysis.

Adopted Methodology for the Cooling Basin/GBRA Storage Water Reservoir

- Embankment fills: employ total unit weight, Φ = 0, and undrained shear strength (i.e., the shear strength intercept at zero pressure on Figure 2.5.5-210 [Line B]).
- Foundation clay strata: (i) for the ”low” embankments, stresses under the embankment load do not bring the foundation clay strata to a fully saturated condition; therefore, employ total unit weights, Φ = 0, and undrained shear strengths corresponding to the applied pressures induced by the embankment; (ii) for the “high” embankments, employ total unit weight, Φ = 0, and undrained shear strengths corresponding to the net applied pressure induced by the embankment (i.e., the shear strength at applied pressure minus generated pore water pressure on Figure 2.5.5-212 [Line C]). As a decisive factor, an embankment is considered “high” if the applied vertical pressure is greater than 5.9 ksf (otherwise the embankment is “low”). Any additional pressure past 5.9 ksf increases the pore water pressure by the same amount.
- Foundation sand strata: employ total unit weight, Φ’ = 40°, and c’ = 0.4 ksf.

2.5.5.2.2.3 Steady-State Seepage Case

For this case, only the outboard slope needs to be analyzed. The steady-state seepage case is nearly always analyzed using the effective stress shear strength parameters (Φ’, c’) assuming that the pore pressures acting are governed by gravity flow nets through the embankment (References 2.5.5-210 and 2.5.5-212). For most well-compacted embankment materials, the effective stress approach is conservative because any shear strains, which may be imposed on the embankment after construction is completed and the reservoir is full, are

likely to cause the soil to dilate and reduce the pore pressures temporarily (Reference 2.5.5-210).

Adopted Methodology for the Cooling Basin/GBRA Storage Water Reservoir

- Use seepage forces and effective stress shear strength parameters.

2.5.5.2.2.4 Rapid Drawdown Case

Both effective stress and total stress methods of analysis can be used to analyze this case. The former requires an estimation of the pore pressures within the slope. This can be done based on gravity flow type of considerations (i.e., by graphical flow nets, or by calculating with finite element or finite differences programs). However, the pore pressure estimates for the rapid drawdown case must be considered as somewhat less reliable than for shortly after construction and steady-state seepage cases (Reference 2.5.5-210).

Adopted Methodology for the Cooling Basin/GBRA Storage Water Reservoir

2.5.5.2.2.5 The total stress analysis adopted consists of several stages. The first stage calculates the effective stresses within the embankment following the steady-state condition. The second stage calculates the undrained shear strengths corresponding to the effective stress throughout the embankment during the steady-state condition. In the third stage, the FOS is calculated based on the undrained shear strengths from the second stage and by employing total unit weights.Slope Deformation During the Design Seismic Event

The Federal Guidelines for Dam Safety (Reference 2.5.5-203) concludes that for a dam and foundation not subject to liquefaction, minor deformation may take place but should not lead to failure if all of the following conditions are satisfied:

- Dam and foundation materials are not subject to liquefaction and do not include loose soils or sensitive clays.
- The dam is well built and compacted to at least 95% of the laboratory maximum dry density, or to a relative density greater than 80%.
- The slopes of the dam are 3H:1V or flatter, and/or the phreatic line is well below the outboard slope of the embankment.

- The peak horizontal acceleration at the base of the embankment is no more than 0.20 g.
- The static factors of safety for all potential failure surfaces (other than shallow surficial slides) are greater than 1.5 under loading and pore pressure conditions expected immediately prior to the earthquake.
- The freeboard at the time of the earthquake is at least 3% to 5% of the embankment height and not less than 3 feet. Freeboard requirements to accommodate reservoir seiche waves or co-seismic movement of faults at the dam site or in the reservoir must be considered as a separate issue.
- There are no critical appurtenant features that would be harmed by small movements of the embankment or that have the potential to cause cracks that allow internal erosion.

If these conditions are not satisfied, then a more detailed study is required. The objective of deformation analysis is to determine whether plausible movements would be sufficient to allow overtopping by the reservoir, or if cracking at critical locations could result in failure by internal erosion. Table 10 in Reference 2.5.5-202 summarizes suggested methods of performing these pseudo-static-screening analyses.

Although the embankment dams of the cooling basin/GBRA storage water reservoir are designed to comply with the conditions defined in *The Federal Guidelines for Dam Safety* (Reference 2.5.5-203), the seismic deformation of the slopes is still estimated.

Adopted Methodology for the Cooling Basin/GBRA Storage Water Reservoir

- The Makdisi/Seed approach (Reference 2.5.5-206) is selected for the evaluation of the earthquake slope deformations of the embankment dams. In this approach, the expected seismic deformation of the slopes is calculated as a function of the pseudo-static yield coefficient of horizontal acceleration that brings the FOS against sliding of the slope down to 1.0, the average effective acceleration within the soil mass, and the duration of strong ground shaking.

2.5.5.2.2.6 Post-Earthquake Stability

Cyclic shear stress applications are known to cause an increase of the pore pressures within a soil mass. Although that increase may be high enough to cause liquefaction of loose granular deposits, its effect on clay

soils is small. Quoting H.B. Seed in his 1979 Rankine Lecture (Reference 2.5.5-209), "There is very clearly a marked difference between the seismic resistance of dams constructed of clayey soils and those constructed of saturated sands or other cohesion-less soils […] It may be also noted in passing that, in general, the peak strength and residual strength for the types of soils used for dam construction do not seem to differ appreciably, although this merits further study." Typical examples of the small reduction of strength (15% to 20%) in clays because of cyclic strain or cyclic stress applications are shown on Figures 11 and 12 of the reference.

Adopted Methodology for Cooling Basin/GBRA Storage Water Reservoir

- Adopt residual undrained shear strengths of the fill materials, foundation clays, and foundation sands equal to 80% of the pre-earthquake strengths shown on Figures 2.5.5-210 (Line B), 2.5.5-212 (Line C), and 2.5.5-213 (Line A), respectively. For foundation sands, use c' = 0.32 ksf (being 80% of the recommended c' = 0.4 ksf [refer to Subsection 2.5.5.1.9.1.3]).

2.5.5.2.2.7 Design Criteria

The following design criteria apply to the cooling basin/GBRA storage water reservoir embankment dams:

- Embankments built with clayey material (representative materials are Composite "A"/Sand, having USCS classification of SC; and Composite "B"/Clay, having USCS classification of CL) taken from site excavations, and compacted to a minimum of 95% of modified Proctor (Reference 2.5.5-217) maximum dry density at about 4% above optimum moisture content. Refer to Subsections 2.5.4.5.3 and 2.5.5.4 and Table 2.5.4-245.
- Geotechnical properties of the embankment fill materials used in the design of the embankments are selected based on laboratory test results from recompacted soils. Refer to Subsections 2.5.4.5.3 and 2.5.5.4 and to Table 2.5.4-245.
- Embankments are designed with slopes 3H:1V, or flatter.
- Horizontal acceleration at the base of the embankments: 0.10g.
- Minimum slope stability static FOSs are as follows (References 2.5.5-202, 2.5.5-210, and 2.5.5-212):
  - End of construction: 1.30

  - Steady-state seepage: 1.50
  - Rapid drawdown: 1.30
  - Pseudo-static: 1.15
- Post-earthquake residual strength: 0.80 x static value.
- Seismic slope deformation: Less than 3 feet.
- Filters: Designed per References 2.5.5-210 and 2.5.5-212.
- Inboard slope protection: Soil-cement, approximately 2.5 feet thick (perpendicular to the slope) or other suitable material as selected at detailed design.

2.5.5.2.3 Analytical Slope Stability and Seepage Models

Slope stability studies are based on models that account for the stratification of the subsurface materials, take into account the pore water pressure distribution (effective stress analyses) or the variation of undrained shear strengths (total stress analyses). Pore water pressure distribution within the embankment dams for the steady-state condition is based on seepage flow nets.

Note that at this preliminary stage of design, subsurface and groundwater conditions along the alignment of the embankment dams are defined by investigations (e.g., borings, CPTs) on plan spacings of 1500 feet center to center. Subsurface and groundwater conditions at locations beyond the outboard toe of the embankment dams (particularly beyond the easternmost dam, i.e., the east dam of the GBRA storage water reservoir) are defined by supplemental investigations. The preliminary engineering analyses reported here, conservatively assume that the groundwater level to distances considerably beyond the outboard toe of the embankment dams lies at the ground surface, an assumption that is unlikely to occur. Under these conservative conditions the analyses indicate that zones of high hydraulic gradient develop at distances away from the toe of the embankment. Supplemental investigations provide the means to analyze this potential occurrence in more detail.

2.5.5.2.4 Computer Codes: Descriptions, Justifications, and Abstracts

Appendix 2.5.5-AA contains the abstracts of the two computer software codes identified below (References 2.5.5-220 and 2.5.5-221).

2.5.5.2.4.1 Slope Stability Analyses

SLOPE/W 2004 (version 6.13) computer software

This code is capable of calculating factors of safety for a variety of slip surface shapes with variable geometry, soil properties, and stratigraphy and under different distributions of pore pressure. The program is used to find the critical slip surfaces and their corresponding FOSs.

2.5.5.2.4.2 Flow Net Construction Analyses

SEEP/W 2004 (version 6.13) computer software

This finite element code analyzes groundwater seepage and excess pore water pressure dissipation problems within porous materials under saturated steady-state problems to unsaturated time-dependent conditions. The code is used to prepare flow nets under steady-state conditions. The results from SEEP/W are exported to SLOPE/W to find the FOS of embankment slopes.

2.5.5.2.5 Assumptions, Considered Cases, and Calculated Factors of Safety

The results of SLOPE/W stability analyses using the Bishop methods of slices are presented for each analysis type. As stated in Reference 2.5.5-220 (pages 81 and 122), finding the position of the critical slip surfaces requires guidance from the analyst. Sometimes, factors of safety can be calculated for unrealistic slips (e.g., very shallow slip surfaces that track the surface of the embankment slope). Then, it becomes the responsibility of the analyst to judge the validity of the particular slip and factor of safety. This means that in some of the cases, the calculated factors of safety are lower than those presented here; however, the slip surfaces presented here represent realistic failure mechanisms.

Figures 2.5.5-213 through 2.5.5-220, Figures 2.5.5-201 through 2.5.5-208, and Table 2.5.5-204 illustrate subsurface conditions and embankment dam heights along the perimeter of the cooling basin/GBRA storage water reservoir. Considering this information, five cross sections selected for slope stability analyses representative of the range of conditions are as follows:

- Cross section at CPT C-2302, (refer to Embankment Profile A, Figure 2.5.4-281): The embankment in this area is adjacent to the power block along the north dam of the cooling basin. Subsurface conditions

consist of inter-layers of clays (Strata Clay 1 [Top], Clay 1 [Bottom], and Clay 3) and sands (Strata Sand 1, Sand 2, and Sand 4). Embankment height is 33 feet (inboard) and 22.5 feet (outboard).

- Cross section at Boring B-2352, (refer to Embankment Profile B, Figure 2.5.4-282): The cross section is at the southeastern corner of the cooling basin. Subsurface conditions consist of alternating layers of clays (Strata Clay 1 [Top], Clay 1 [Bottom], and Clay 3) and sands (Strata Sand 2, Sand 4, Sand 5, and Sand 6) (note that the figure in this particular instance is truncated such that the deeper soils strata are not completely illustrated). Embankment height is 39.1 feet (inboard and outboard). As such, this cross section is representative of a typical-height basin/reservoir embankment with predominantly sand foundation conditions.
- Cross section at Boring B-2333, (refer to Embankment Profile C, Figure 2.5.4-283): The cross section is on the west embankment of the cooling basin. Subsurface conditions consist primarily of clays (Strata Clay 1 [Top], Clay 1 [Bottom], Clay 3, and Clay 5 [Top]) with two sand layers (Strata Sand 2 and Sand 4). Embankment height is 33 feet (inboard) and 25.9 feet (outboard). As such, this cross section is representative of a typical-height basin/reservoir embankment, with predominantly clay foundation conditions.
- Cross section at Cone Penetration Test C-2317, (refer to Embankment Profile D, Figure 2.5.4-284): The cross section is along the east embankment of the GBRA storage water reservoir where the ground surface is lowest. Subsurface conditions are primarily sands (Strata Sand 2, Sand 4, and Sand 5) with two thin clay layers (Strata Clay 1 [Bottom] and Clay 3). Embankment height is 56.8 feet (inboard and outboard). As such, this cross section is representative of a maximum-height basin/reservoir embankment, with predominantly sand foundation conditions.
- Cross section at Boring B-2353, (refer to Embankment Profile E, Figure 2.5.4-285): The cross section is at the southeastern corner of the GBRA storage water reservoir. Subsurface conditions consist primarily of sands (Strata Sand 1, Sand 2, and Sand 4) with some inter-layered clays (Strata Clay 1 [Top], Clay 1 [Bottom], and Clay 5 [Top]). Embankment height is 36.4 feet (inboard and outboard). As

such, this cross section is representative of a typical-height basin/reservoir embankment, with predominantly sand foundation conditions.

The stability of each cross section is analyzed under the five cases outlined in Subsection 2.5.5.2.2.1.

Geotechnical soil properties for the stability analyses are those presented in Subsection 2.5.5.1.9.

The analyses are based on the following assumptions:

- Dam Crest: elevation 102 feet (NAVD 88)
- Bottom of Basin/Reservoir: elevation 69 feet (NAVD 88)
- Maximum Water Level: elevation 96 feet (NAVD 88) (for slope stability analyses) (note that normal maximum operating water level is 91.5 feet (NAVD 88))
- Freeboard: 6 feet
- Drawdown: variable; 6 feet below embankment crest
- Design ground surface acceleration: 0.10g associated with a moment magnitude 7.6 characteristic earthquake

2.5.5.2.5.1 Shortly After Construction Case

Critical slip surfaces are shown on Figures 2.5.5-214 through 2.5.5-218. Calculated factors of safety are shown in Table 2.5.5-205. In all cases the calculated factors of safety exceed the minimum design factor of safety of 1.3.

2.5.5.2.5.2 Steady-State Seepage Case

Critical slip surfaces are shown on Figures 2.5.5-219 through 2.5.5-223. Calculated factors of safety are shown in Table 2.5.5-206. In all cases the factors of safety exceed the minimum design factor of safety of 1.5.

(Note that an outboard berm, 30 feet wide with top elevation 75 feet (NAVD 88), is required along the east and south cooling basin/GBRA storage water reservoir embankment dams, to achieve the minimum slope stability FOS of 1.50 for the steady-state seepage cases. Refer to Embankment Profiles B, D, and E [Figures 2.5.4-282, 2.5.4-284, and 2.5.4-285, respectively].)

2.5.5.2.5.3 Rapid Drawdown Case

Critical slip surfaces are shown on Figures 2.5.5-224 through 2.5.5-228. Calculated factors of safety are shown in Table 2.5.5-207. In all cases the calculated factors of safety exceed the minimum design factor of safety of 1.3.

Note that an inboard berm, approximately 100 feet wide with top elevation of 69 feet (NAVD 88), is required at the maximum-height embankment areas along the east GBRA storage water reservoir embankment dam, to achieve the minimum slope stability FOS of 1.30 under the rapid drawdown case. Refer to Embankment Profile D (Figure 2.5.4-284).

Note also that over-excavation of the foundation clay (Stratum Clay 1 [Top]) and the foundation sand (Stratum Sand 1) is required along the north cooling basin embankment dam adjacent to the power block, to achieve the minimum slope stability FOS of 1.30 under the rapid drawdown case. Refer to Embankment Profile A (Figure 2.5.4-281).

2.5.5.2.5.4 Seismic Stability and Post-Earthquake Deformations

The Makdisi/Seed approach (Reference 2.5.5-206) is selected from the table in Reference 2.5.5-202 for the evaluation of earthquake-induced slope deformations of embankment dams. In this approach, the expected seismic deformations of the slopes are calculated as a function of the following:

- The pseudo-static yield coefficient of horizontal acceleration that brings the factor of safety against sliding of the slope down to 1.0
- The average effective acceleration within the soil mass
- The ratio of the yield acceleration to the average effective embankment acceleration
- The duration of strong ground shaking

Preliminary design criteria call for an earthquake characterized by peak ground acceleration equal to 0.10g at the base of the embankment dam associated with a moment magnitude 7.6 earthquake.

Critical slip surfaces and yield accelerations are shown on Figures 2.5.5-229 through 2.5.5-233 and are summarized in Table 2.5.5-208.

The average effective ground acceleration within the embankment dam is a function of the amplitude of the ground acceleration at the crest of the

embankment. The maximum value of the crest acceleration is a function of several variables, namely: embankment height, fill stiffness, and characteristics of the earthquake ground motion. Experience shows that the ratio of crest acceleration to ground surface acceleration at the base of the embankment may range between less than 1 to about 2. A conservative value of the ratio equal to 2 is adopted for the slope deformation evaluations. Figure 9 in Reference 2.5.5-206 shows that the average effective embankment acceleration is equal to about 45% the crest acceleration. Consequently, the average effective embankment acceleration in this case is equal to: ground acceleration at the base of the embankment (0.10g) x crest amplification factor (2) x reduction factor between crest and average effective embankment acceleration (0.45) = 0.09g.

Table 2.5.5-209 lists the values of the yield acceleration/maximum average embankment acceleration ratios for the five embankment sections. Figure 14 in the Makdisi/Seed reference (Reference 2.5.5-206) shows that the expected seismic displacements for the listed ratios are negligible.

Post-earthquake slope stabilities are presented on Figures 2.5.5-234 through 2.5.5-238 and are summarized in Table 2.5.5-210 (outboard slope). In all cases the calculated factors of safety exceed 1.5.

2.5.5.2.6 Liquefaction Evaluation

Refer to Subsection 2.5.4.8, which concludes that the liquefaction potential of VCS site soils is not an issue with respect to both the safety-related power block and the nonsafety-related cooling basin/GBRA storage water reservoir. As noted above, a peak horizontal ground surface acceleration of 0.10g and a moment magnitude 7.6 characteristic earthquake are employed (refer to Subsection 2.5.4.7.5).

2.5.5.2.7 Settlement Analyses

Estimated foundation settlements under the weight of the embankment dams are based on a simplified and conservative assumption of the elastic moduli of the various strata. Results of the analyses show:

- 60-foot-high embankment dams (i.e., the maximum height embankment dams) have 12 inches of settlement under the crest and 3 to 4 inches of settlement under the toes.

- 40-foot-high embankment dams (i.e., the typical height embankment dams) have 7 inches of settlement under the crest and 2 to 3 inches of settlement under the toes.

Analyses are also made to estimate the compression of the 60-foot high and 40-foot high embankment dams because of self-weight. In both cases, the estimated settlement is less than 1 inch.

2.5.5.3 Logs of Borings

Refer to Subsection 2.5.5.1.5 (Subsurface Investigation) and Subsection 2.5.5.1.9 (Laboratory Testing).

2.5.5.4 Compacted Fill

2.5.5.4.1 General

This section describes: required excavations and backfill volumes, construction materials, construction methods, earthwork controls, and quality assurance/quality controls during and after construction of the embankment dams.

2.5.5.4.1.1 Excavation

Figure 2.5.4-280 is a plan view of the cooling basin/GBRA storage water reservoir showing the locations of the embankment profiles presented on Figures 2.5.4-281 through 2.5.4-285. These figures and the horizontal cross sections on Figures 2.5.5-201 through 2.5.5-208 show the extent of required excavations.

The upper foot of material excavated at the cooling basin/GRBA storage water reservoir area is moderately organic (topsoil), and is removed and reused for site landscaping purposes, or is stockpiled onsite. The base elevation of the basin/reservoir is at 69 feet (NAVD 88); therefore, excavation within the basin/reservoir footprint is accomplished in areas approximately as shown in plan on Figure 2.5.4-280.

In addition, Subsurface Profile G shown on Figure 2.5.4-216 (also shown in plan on Figure 2.5.4-213) along the east dam of the GBRA storage water reservoir shows limited areas of relatively loose granular materials having SPT $(N_1)_{60}$ less than 10 blows per foot at shallow depths below the surface, as follows:

- Boring B-2306A: uppermost 1.5 feet (elevation 64.3 feet [NAVD 88] to elevation 62.8 feet [NAVD 88]) has SPT $(N_1)_{60}$ of 9 blows per foot (bpf) (Stratum Sand 1).

- Boring B-2315: uppermost 1.5 feet (elevation 47.1 feet [NAVD 88] to 45.6 feet (NAVD 88)) has SPT $(N_1)_{60}$ of 8 bpf (Stratum Sand 1).
- Boring B-2322: uppermost 1.5 feet (elevation 68.5 feet [NAVD 88] to elevation 67.0 feet [NAVD 88]) has SPT $(N_1)_{60}$ of 9 bpf (Stratum Sand 1).

Also, as noted in Subsection 2.5.4.8.3.2, cone penetration test C-2308: uppermost 5.25 feet (elevation 58.02 feet [NAVD 88] to elevation 52.77 feet [NAVD 88]) is potentially liquefiable by the CPT method (Stratum Sand 1).

The relatively loose materials occurring in these areas are removed or recompacted as a matter of dam foundation preparation.

2.5.5.4.1.2 Backfill

Overall, at the cooling basin/GBRA storage water reservoir, current estimates are that approximately 28 million cubic yards of material are moved during earthwork to establish site grades, comprised of 20 million cubic yards of clay to construct the embankment dams and internal dikes, 1 million cubic yards of sand (from off site sources) for a sand drainage blanket at the outside toe of the embankment dams and 7 million yards of top soil that will be moved to a spoils area or throughout the site to reestablish vegetation in disturbed areas.

As stated above, the bottom of the cooling basin/GBRA storage water reservoir is elevation 69 feet (NAVD 88), with limited areas along the east dam of the GBRA storage water reservoir at lower elevations. Backfilling within the footprint of the basin/reservoir (i.e., inboard of the inboard toe of the embankment) is additionally required in certain of the lower elevation areas, especially along the east embankment dam of the GBRA storage water reservoir at the highest embankment sections. In these limited areas an inboard berm is constructed to elevation 69 feet (NAVD 88) (refer to embankment profile D shown on Figure 2.5.4-284 [also shown in plan on Figure 2.5.4-280]), ensuring stability of the inboard embankment slope in the rapid drawdown case.

2.5.5.4.1.3 Construction Materials: Earth Dams and Drainage Materials

2.5.5.4.1.3.1 Exploration and Field Studies

The excavated area of the cooling basin/GBRA storage water reservoir (refer to Figure 2.5.4-280), being the source of fill materials for

embankment dams, is explored in the field by 34 (of 60 total) borings; 12 (of 27 total) CPTs, and 8 (of 12 total) test pits. The locations of borings, CPTs, and test pits are shown on Figure 2.5.4-202 and are summarized in Table 2.5.4-202. Drilling and sampling procedures, as well as the logs of borings and test pits, are described in Subsection 2.5.4.2.2 and are contained in Appendix 2.5.4-B. CPT methodology and results are also described in Subsection 2.5.4.2.2, with detailed records contained in Appendix 2.5.4-B.

2.5.5.4.1.3.2 Material Sources

Fill material for embankment dam construction is obtained from the excavated area within the footprint of the basin/reservoir (refer to Figure 2.5.4-280), and from adjacent areas if required. Two types of construction materials are used, identified in test results as Composite “A” (an excavated sand material) and Composite “B” (an excavated clay material). Particle size constituents and compaction characteristics of these two materials are presented in Table 2.5.4-245.

Drainage sand materials for the construction of drainage blankets are obtained from off-site sources (refer to Subsection 2.5.4.5.1 for additional detail). Properties of these granular materials are presented in Table 2.5.4-233.

2.5.5.4.1.3.3 Static and Dynamic Properties of Materials

A comprehensive laboratory test program is accomplished to define the general physical, strength, compressibility, and dynamic properties of the embankment fill materials (i.e., Composite “A” materials and Composite “B” materials). Tests include:

- Physical properties: USCS classification, natural moisture content, unit weight, specific gravity, Atterberg limits, grain size distribution, organic content, and moisture-density relationships.
- Strength and compressibility properties (measured on samples prepared at 95% of the modified Proctor [Reference 2.5.4-217] maximum dry densities [plus or minus 1 pcf], compacted at moisture contents equal to 4% above the optimums [plus or minus 0.5 %]): isotropically-consolidated undrained (CIU) triaxial compression tests, direct simple shear tests, RCTS tests, and consolidation tests.

Tests methods, results, and interpretations are presented in Subsection 2.5.4.2 and Subsection 2.5.5.1.9.

With respect to the dynamic properties of embankment fill materials, note that the measured shear moduli (G_{max}), from RCTS testing, and at approximately 10^{-4} percent shear strain, for Composite “A” and Composite “B” materials are approximately 5700 ksf and 3700 ksf, respectively (reference Appendix 2.5.4-B). These values correspond to shear wave velocities (V_s) for Composite “A” and Composite “B” materials of approximately 1160 feet per second and 945 feet per second, respectively.

Tests to define the geotechnical properties of drainage sand materials similarly include:

- Physical properties: USCS classification moisture content, specific gravity, grain size distribution, and moisture-density relationships.
- Strength properties (obtained on samples prepared at 95% of the modified Proctor [Reference 2.5.4-217] maximum dry densities [plus or minus 1 pcf], compacted at moisture contents equal to the optimums [plus or minus 0.5 %]): direct shear tests only.

Tests methods, results, and interpretations are presented in Subsections 2.5.4.2 and 2.5.5.1.9.

2.5.5.4.1.3.4 Quantities

Refer to Subsection 2.5.5.4.1.2 for estimated quantities of construction materials resulting from site grading.

2.5.5.4.2 Compaction of Backfill and Drainage Materials

Technical specifications are prepared at project detailed design covering:

- Preparation of subgrades for areas to receive fills
- Conditioning to required moisture and processing to obtain a uniform fill material
- Handling of processed fill material
- Equipment used for compaction
- Fill placement procedures, including thickness of uncompacted lifts, number of compactor passes/coverages, and compaction equipment operational requirements
- Acceptability of drainage and slope protection materials, and placement procedures
- Testing requirements

- Embankment instrumentation materials, installation, monitoring, and reporting
- Record keeping and quality assurance/quality control procedures

2.5.5.4.3 Construction Methods

Considering the large volume of embankment fill used to construct cooling basin/GBRA storage water reservoir embankment dams, a more complete understanding of the best method for placing embankment fill materials has considerable cost advantages. As such, plans for a surveyed trial fill are prepared at project detailed design.

The location of the trial fill is selected along one of the interior dikes of the cooling basin such that it may form part of the final cooling basin construction.

The trial fill provides valuable data from which the optimum selection of the following factors can be made:

- Optimum compaction equipment type
- Thickness of uncompacted lifts
- Number of compactor passes/coverages
- Compaction equipment speed
- Embankment fill placement moisture content

2.5.5.4.4 Earthwork Controls

Embankment dam construction is controlled to verify that the as-placed engineering properties of embankment fill materials are at least equal to the values assumed in design. Regular testing is required, as follows:

- Identification and control of fill materials prior to placement, including: laboratory moisture/density relationships, grain size analyses, and Atterberg limits.
- Control of the embankment fills initially carried out by visual evaluation, including: the uniformity of the material itself, as delivered to the embankment fill area; the uniformity of the moisture content; the thickness of the uncompacted and compacted lifts; and the adequate equipment performance in compacting fills.
- Control of the thickness of as-compacted lifts accomplished via frequent leveling surveys.

- In situ field density by the sand replacement method and/or the nuclear gauge method. Note that in the case of the nuclear gauge, the instrument is calibrated using the standard calibration block at least twice per day, and also verified by comparison with immediately adjacent sand replacement tests once per week.
- In situ field moisture content by various methods, including: oven drying, nuclear gauge, microwave oven, or hot plate/direct heating. All methods are calibrated by comparison with oven drying as a standard.

2.5.5.4.5 Quality Assurance/Quality Control Measures During and After Construction

A field manual is prepared to ensure that the field engineer and inspection staff understand the construction procedures and record-keeping requirements for the earthwork fieldwork. The required competence of the personnel and the number of inspection staff assigned to the construction of the embankment dams are also identified in the manual.

Inspectors prepare daily reports covering the activities for their shifts. The reports contain: progress of construction, tests assigned, test results reported, and instructions for the inspector about to go on shift. Appropriate job-specific forms are prepared for the format of the daily report.

The chief field engineer prepares periodic progress reports, which are the means of transmitted field information and data to the project engineer. The progress reports include the following:

Fill material description: material types and natural moisture contents.

Embankment fill operations: documentation of equipment used, moisture conditioning and placement operations, and compaction methods and lift thicknesses.

Photographs: documenting activities in the material excavations, stockpiles, and embankment fill areas.

Tests: results of tests carried out during the reporting period (both laboratory and in situ)

Compaction equipment: types and manufacturers' specifications

The chief field engineer prepares a final embankment construction report covering: construction materials, construction history, equipment

employed, and summarizing quality assurance/quality control test results (both laboratory and in situ).

Cooling basin/GBRA storage reservoir embankment dams are additionally monitored during and after construction for, among other things:

- Groundwater levels, especially outboard of the embankment dams following construction
- Pore water pressures occurring within embankment fills
- Embankment settlements

A detailed instrumentation and monitoring program is prepared at project detailed design.

2.5.5.5 References

2.5.5-201 U.S. NRC, Office of Nuclear Regulatory Research, *Combined License Application for Nuclear Power Plants* (LWR Edition), Regulatory Guide 1.206, June 2007

2.5.5-202 Duncan, J.M., and S.G. Wright, *Soils Strength and Soil Stability*, John Wiley and Sons, Inc., New Jersey, 2005.

2.5.5-203 Federal Emergency Management Agency (FEMA), “Federal Guidelines for Dam Safety,” *Earthquake Analyses and Design of Dams*, May 2005.

2.5.5-204 Justin J.D., Hinds, J. and W.P. Creager, *Engineering for Dams*, vol. III, John Wiley and Sons, Inc., New York, 1945.

2.5.5-205 Ladd, C.C. and DeGroot, D.J., “Recommended Practice for Soft Ground Site Characterization: Arthur Casagrande Lecture,” *12th Pan-American Conference on Soil Mechanics and Geotechnical Engineering*, Massachusetts Institute of Technology, Cambridge, Massachusetts, 2003.

2.5.5-206 Makdisi, F.I. and Seed, H.B., “A Simplified Procedure for Estimating Earthquake-Induced Deformations,” *Dams and Embankments*, Report No. UCB/EERC-77/19, University of California, Berkeley, California, August 1977.

2.5.5-207 Middlebrooks, J.G., “Earth Dam Practice in the United States,” *Transactions*, American Society of Civil Engineers (ASCE), Centennial Volume, 1953.

2.5.5-208 Seed, H.B., Makdisi, F.I., and de Alba, P., *The Performance of Earth Dams during Earthquakes*, Report No. UCB/EERC-77/20, University of California, Berkeley, CA, August 1977.

2.5.5-209 Seed, H.B., "Considerations in the Earthquake-Resistance Design of Earth and Rock Fill," *The 19th Rankine Lecture, Geotechnique*, v. 29, No. 3, 1979.

2.5.5-210 Sherard, J.L., Woodward, R.J., Gizienski, S.F., and W.A. Clevenger, *Earth and Earth-Rock Dams*, John Wiley and Sons, Inc., NJ, 1963.

2.5.5-211 Sherard, J.L., Dunnigan L.P., and J.R. Talbot, *Filters for Silts and Clays*, Special Publication No 3, American Society of Civil Engineers, 1992.

2.5.5-212 US Army Corps of Engineers, *Engineering and Design Slope Stability Analysis Manual*, EM 1110-2-1902, October 31, 2003.

2.5.5-213 Kulhawy, F.H., and P.W. Mayne, *Manual on Estimating Soil Properties for Foundation Design*, Research Project 1493-6, Cornell University, Ithaca, NY, 1990.

2.5.5-214 Vaid, Y.P., and R.G. Campanella, "Triaxial and Plane Strain Behavior of Natural Clay," *Journal of the Geotechnical Engineering Division*, vol. 100, no. GT3, ASCE, March 1974.

2.5.5-215 Lewis, M.R., e-mail to I. Arango, July 10, 2008.

2.5.5-216 Taylor, D.W., *Fundamentals of Soil Mechanics*, John Wiley and Sons, Inc., New York, 1956.

2.5.5-217 Terzaghi, K., Peck, R.B., and Mesri, G., *Soil Mechanics in Engineering Practice*, John Wiley and Sons, Inc., New York, 1996.

2.5.5-218 Bishop, A.W. and D.J. Henkel, *The Measurement of Soil Properties in the Triaxial Test*, Edward Arnold, 1957.

2.5.5-219 Becker, E., Chan, C.K., and Seed, H.B., *Strength and Deformation Characteristics of Rock Fill Materials in Plane Strain and Triaxial Compression Tests*, Report No. TE 72-3, Department of Civil Engineering, University of California, Berkeley, California, 1972.

2.5.5-220 Krahn J., *Stability Modeling with SLOPE/W: An Engineering Methodology*, First Edition, Rev. 1, Geo-Slope International, Ltd., August 2004.

2.5.5-221 Krahn J., *Seepage Modeling with Seep/W: An Engineering Methodology*, First Edition, Geo-Slope International, Ltd., May 2004.

Table 2.5.5-201
Soil Strata Total Unit Weights

Stratum	Number of Tests	Average Total Unit Weight (pcf)	Values for Use (pcf)
Clay 1(Top)	11	126.1	125[a]
Sand 1	4	121.8	126
Clay 1 (Bottom)	5	122.6	125[a]
Sand 2	3	122.5	126
Clay 3	12	122.9	123
Sand 4	7	122.7	123
Clay 5 (Top)	8	124.6	125[a]
Sand 5	1	116.9	123
Clay 5 (Bottom)	—	—	125[a]
Sand 6	—	—	123[b]
Clay 7	—	—	125[b]
Sand 8	—	—	123[b]
Clay 9	—	—	125[b]
Sand 10	—	—	123[b]
Clay 11	—	—	125[b]

Notes:

[a]Clay 1 (Top) and Clay 1 (Bottom) are assumed to have the same total unit weight. Clay 5 (Top) and Clay 5 (Bottom) are similarly assumed to have the same total unit weight

[b]Unit weight measurements for soil strata below Stratum Sand 5 are not available. For these deeper strata, the results of similar strata were used as follows: for Strata Sand 6, Sand 8, and Sand 10 the results from Stratum Sand 5 are used; and for Strata Clay 7, Clay 9 and Clay 11, the results from Stratum Clay 5 are used

Table 2.5.5-202
Strength Parameters: Embankment Fill (Composite A Sand and Composite B Clay); Foundation Sands; and Foundation Clays

Shortly After Construction Case[a]	
Stratum	Geotechnical Properties
Embankment Fill	s_u=1280 psf, ϕ'=0°, γ=134 pcf
Foundation Clays	τ/σ=0.46, s_{umin}=670 psf, ϕ'=0°, γ=126 pcf Also, for C-2317: s_u=2000 psf, ϕ'=0°, γ=126 pcf
Foundation Sands	s_u=400 psf, ϕ'=40°, γ=126 pcf
Steady-State Seepage Case[a, b]	
Stratum	Geotechnical Properties
Embankment Fill	s_u=0 psf, ϕ'=30°, γ=134 pcf
Foundation Clays	s_u=0 psf, ϕ'=28°, γ=126 pcf
Foundation Sands	s_u=400 psf, ϕ'=40°, γ=126 pcf
Rapid Drawdown Case[a]	
Stratum	Geotechnical Properties
Embankment Fill	τ/σ=0.78, s_{umin}=1280 psf, ϕ'=0°, γ=134 pcf Also, for C-2317: τ/σ=0.70
Foundation Clays	τ/σ=0.46, s_{umin}=670 psf, ϕ'=0°, γ=126 pcf
Foundation Sands	s_u=400 psf, ϕ'=40°, γ=126 pcf
Post Earthquake Case[a]	
Stratum	Geotechnical Properties
Embankment Fill	τ/σ=0.62, s_{umin}=1030 psf, ϕ'=0°, γ=134 pcf Also, for C-2317 : τ/σ=0.56
Foundation Clays	τ/σ =0.36, s_{umin}=530 psf, ϕ'=0°, γ=126 pcf
Foundation Sands	s_u=320 psf, ϕ'=33°, γ=126 pcf

Notes:

[a]The profile at cone penetration test C-2317 represents a “high” embankment (refer to Subsection 2.5.5.2.2.2 for additional detail). Strength values vary slightly for this profile due to relatively high applied vertical pressures (i.e., greater than 5.9 ksf)

[b]The case of “slope deformation during the design seismic event” uses the same strength parameters as the “steady-state seepage case,” to solve for the yield acceleration of each profile

Table 2.5.5-203
D_{85} Particle Sizes: Embankment Fill (Composite A and Composite B); Foundation Sands; and Foundation Clays

Material	D_{15} (mm)	D_{85} (mm)	D_{15}/D_{85}
Filter (Drainage Sand)	0.26	—	—
Embankment Fill (Composite “A”/Sand)	—	0.25	1.0
Embankment Fill (Composite “B”/Clay)	—	0.14	1.9
Foundation Sand (Stratum Sand 1)	—	0.10-0.60	2.6-0.4
Foundation Clay (Stratum Clay 1 [Top])	—	0.08-0.25	3.3-1.0

Table 2.5.5-204
Embankment Dam Heights

Section Considered	Ground Surface Elevation[b] (feet)	Dam Crest Elevation[b] (feet)	Height of Embankment Outboard (feet)	Basin Excavation Inboard (feet)	Height of Embankment Inboard[a] (feet)
B-06	79.0	102.0	23.0	10.0	33.0
B-2302	80.0	102.0	22.0	11.0	33.0
B-2304	68.1	102.0	33.9	None	33.9
B-2315	47.1	102.0	54.9	None	54.9
B-2317	76.7	102.0	25.3	7.7	33.0
B-2318	75.3	102.0	26.7	6.3	33.0
B-2322	68.5	102.0	33.5	None	33.5
B-2333	76.1	102.0	25.9	7.1	33.0
B-2351	63.7	102.0	38.3	None	38.3
B-2352	62.9	102.0	39.1	None	39.1
B-2353	65.6	102.0	36.4	None	36.4
B-2354	76.8	102.0	25.2	7.8	33.0
C-2302	77.5	102.0[b]	22.5[c]	8.5	33.0
C-2308	58.0	102.0	44.0	None	44.0
C-2317	45.2	102.0	56.8	None	56.8

a. On the inboard side, embankment height includes the depth of inboard berm fill

b. The top of the outboard slope of interest to slope stability analysis at C-2302 is 100.0 feet (NAVD 88)

Table 2.5.5-205
Slope Stability Summary, Shortly After Construction Case

Section Analyzed	Factor of Safety Inboard (Bishop Method)	Factor of Safety Outboard (Bishop Method)
B-2333	2.68	2.55
B-2352	2.48	2.44
B-2353	2.61	2.55
C-2302	2.70	2.73
C-2317	1.80	2.00

Table 2.5.5-206
Slope Stability Summary; Steady-State Seepage Case

Section Analyzed	Factor of Safety (Bishop Method)
B-2333	1.79
B-2352	1.80
B-2353	1.94
C-2302	1.72
C-2317	2.10

Table 2.5.5-207
Slope Stability Summary; Rapid Drawdown Case

Section Analyzed	Factor of Safety (Bishop Method)
B-2333	1.75
B-2352	1.68
B-2353	2.17
C-2302	1.54
C-2317	2.09

Table 2.5.5-208
Slope Stability Summary; Yield Accelerations

Section Analyzed	Horizontal Yield Acceleration (g) (Bishop Method)
B-2333	0.26
B-2352	0.18
B-2353	0.29
C-2302	0.22
C-2317	0.30

Table 2.5.5-209
Earthquake-Induced Deformations

Section Analyzed	Ground Surface El. (feet)[a]	Embankment Height (feet)	K_y/K_{max}[b]	Expected Deformation
B-2333	76.1	25.9	0.26/0.09	Negligible
B-2352	62.9	39.1	0.18/0.09	Negligible
B-2353	65.6	36.4	0.29/0.09	Negligible
C-2302	77.5	22.5	0.22/0.09	Negligible
C-2317	45.2	56.8	0.30/0.09	Negligible

a. Elevations are referenced to NAVD 88

b. K_y = yield acceleration, K_{max} = maximum average embankment acceleration

Table 2.5.5-210
Slope Stability Summary; Post-Earthquake Case; Outboard Slope

Section Analyzed	Factor of Safety (Bishop Method)
B-2333	1.74
B-2352	1.61
B-2353	2.24
C-2302	2.13
C-2317	2.05

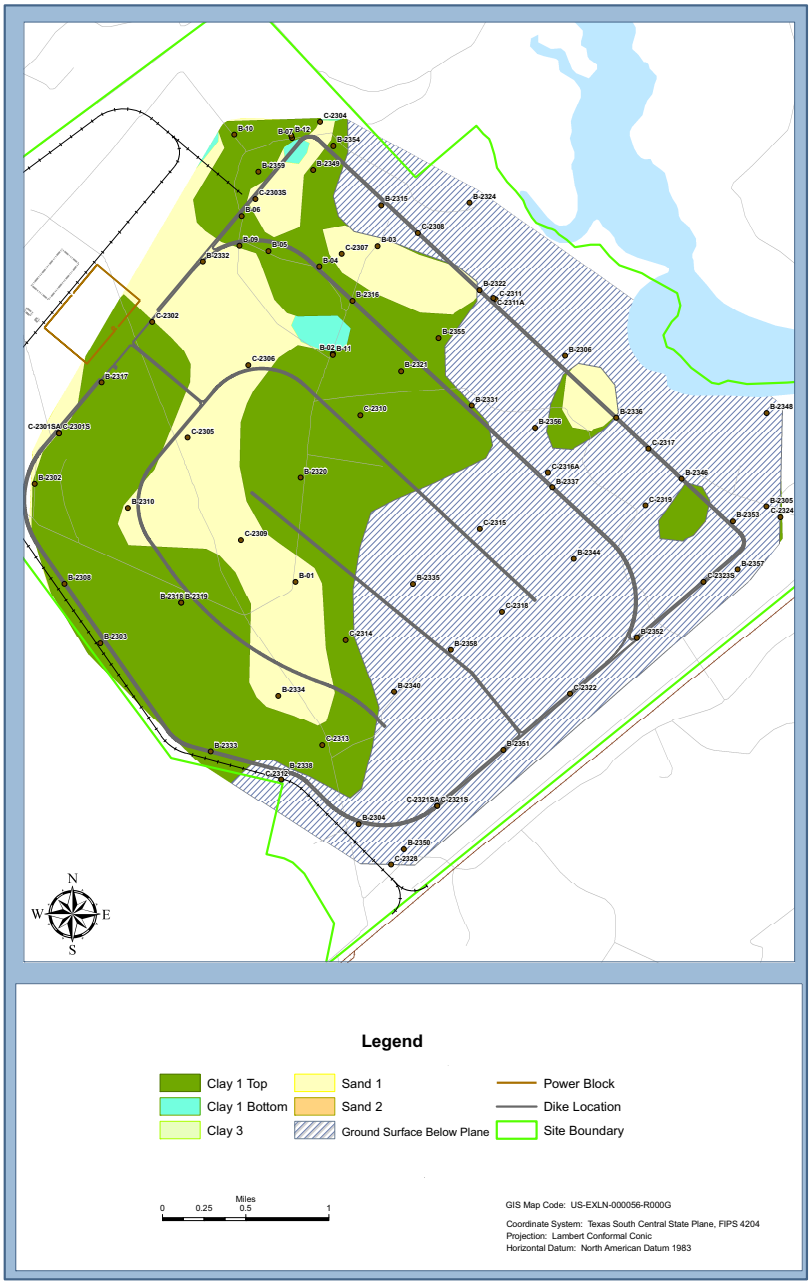

Figure 2.5.5-201 Subsurface Stratigraphy; Elevation 69 Feet (NAVD 88) (Cooling Basin/GBRA Storage Water Reservoir Base Level)

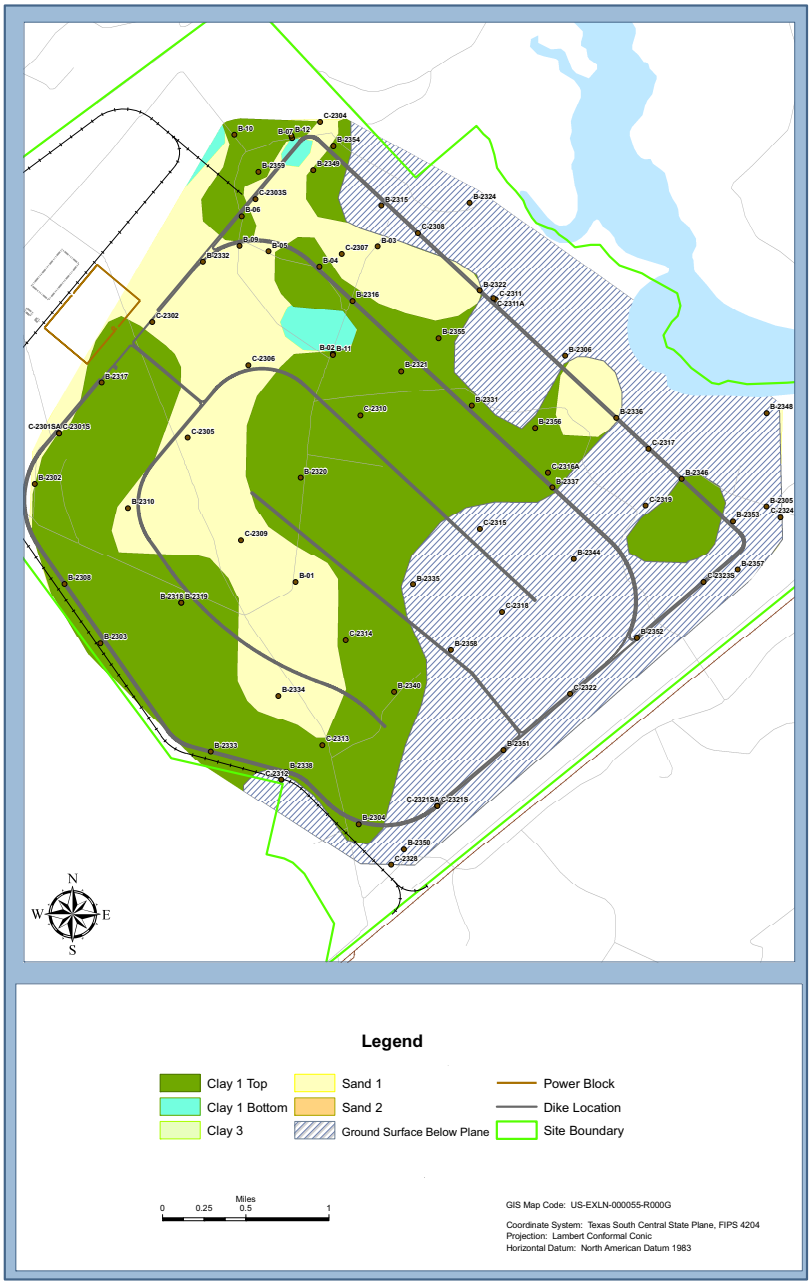

Figure 2.5.5-202 Subsurface Stratigraphy; Elevation 67 Feet (NAVD 88)

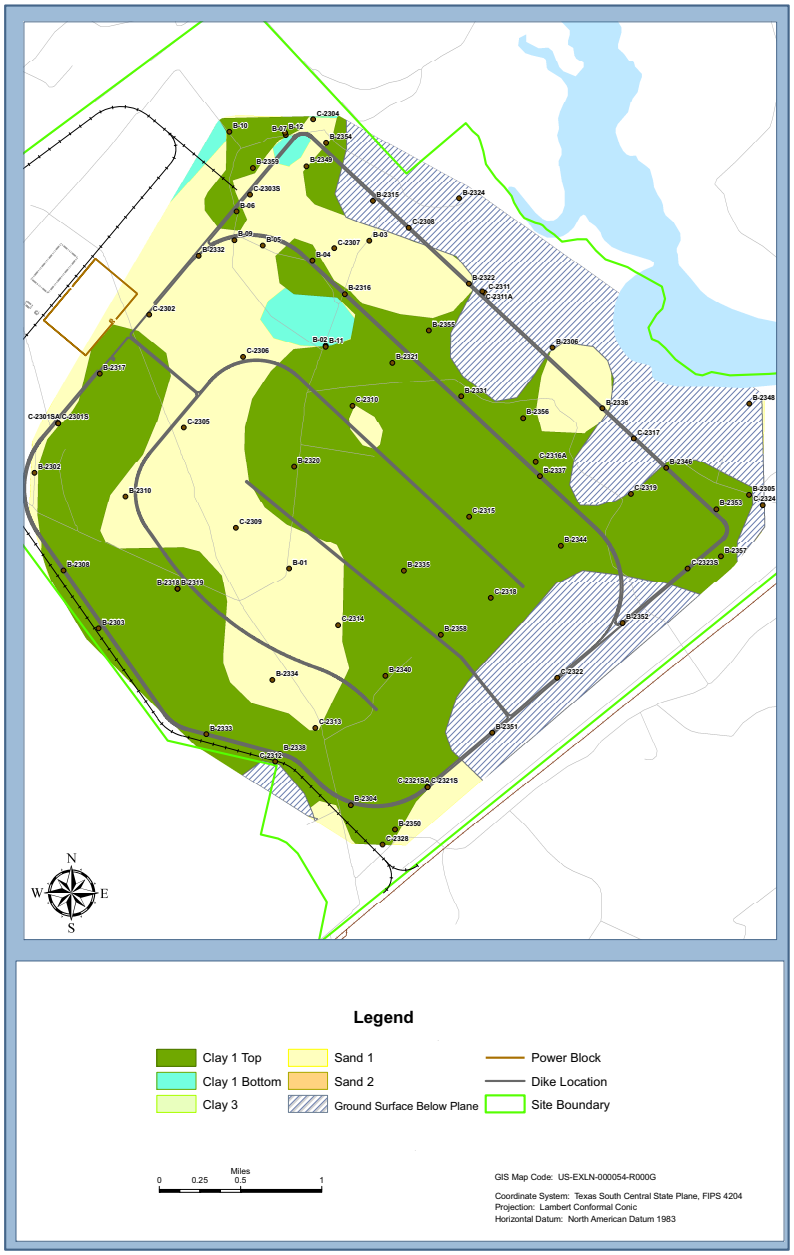

Figure 2.5.5-203 Subsurface Stratigraphy; Elevation 65 Feet (NAVD 88)

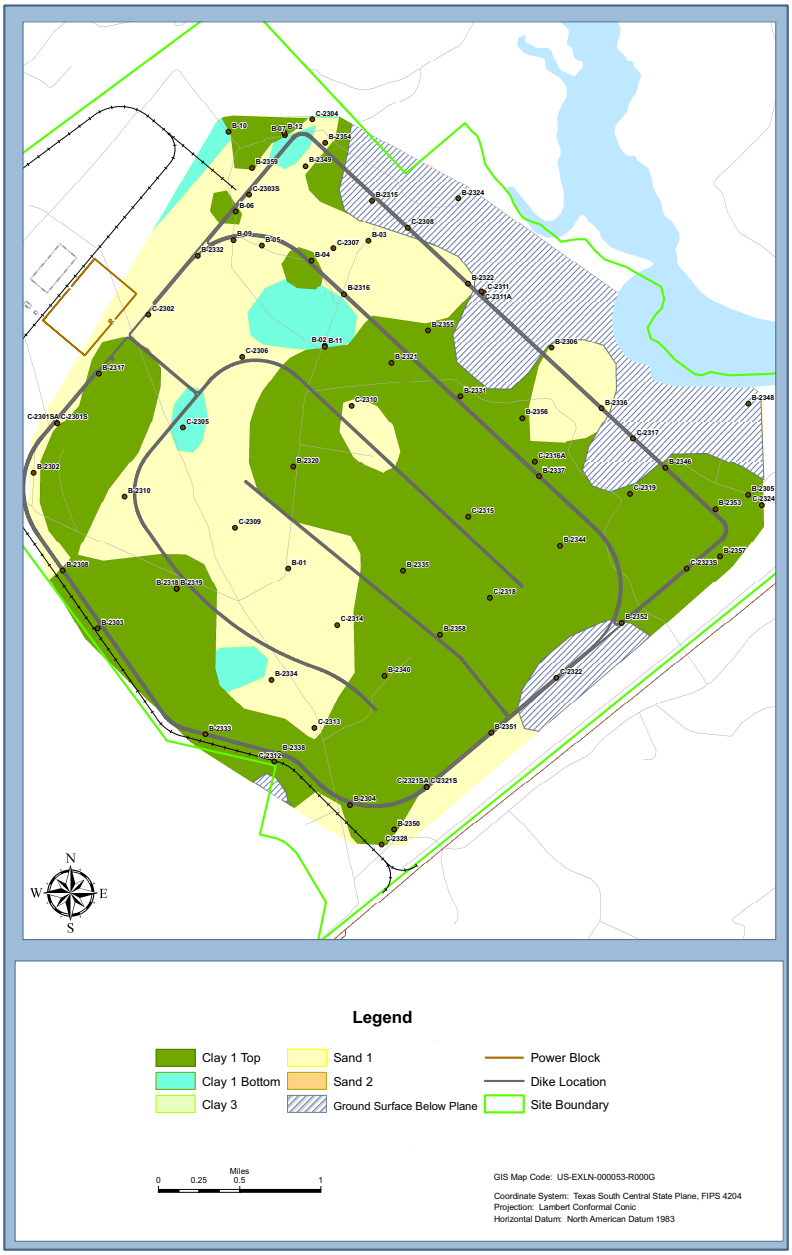

Figure 2.5.5-204 Subsurface Stratigraphy; Elevation 63 Feet (NAVD 88)

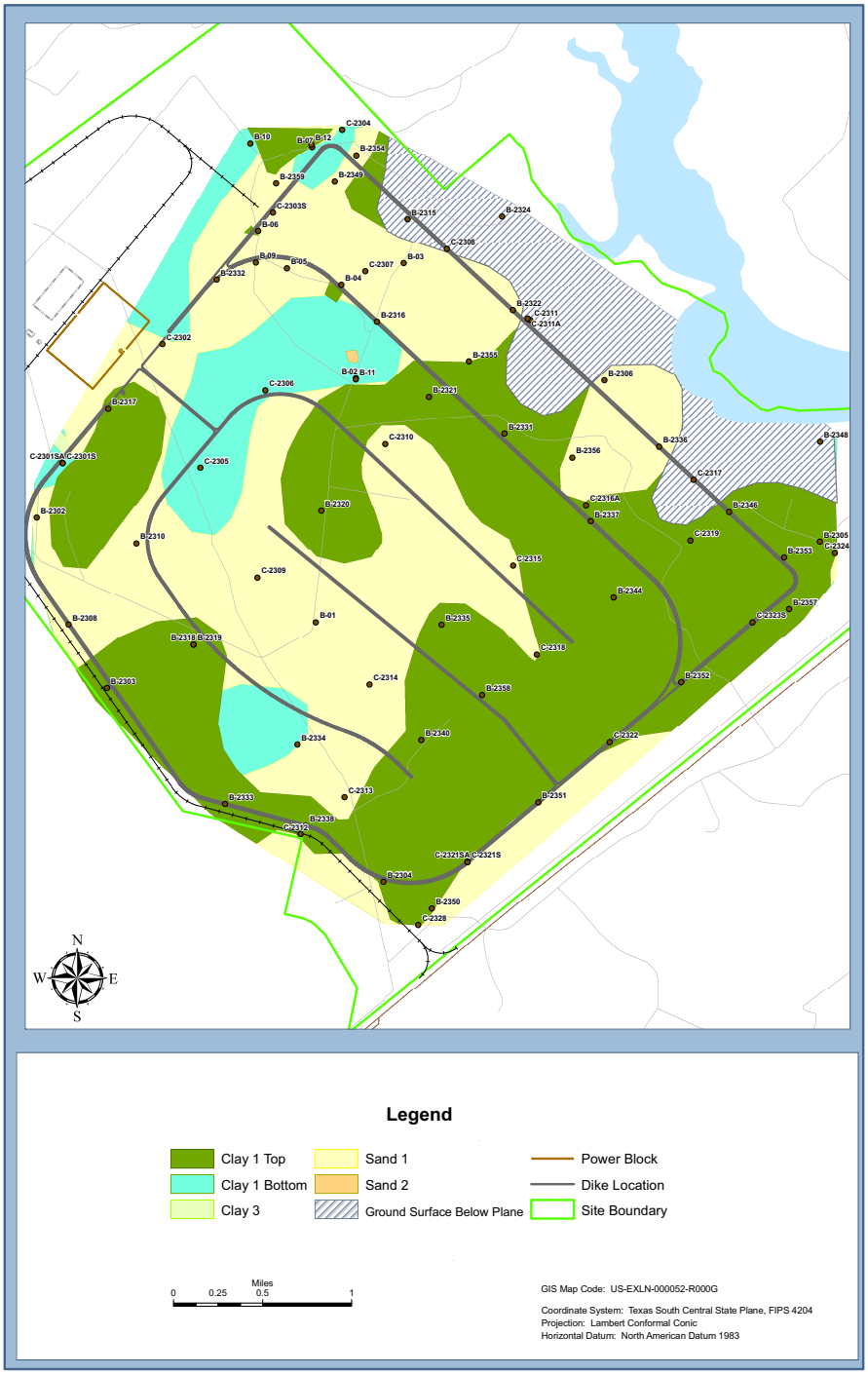

Figure 2.5.5-205 Subsurface Stratigraphy; Elevation 60 Feet (NAVD 88)

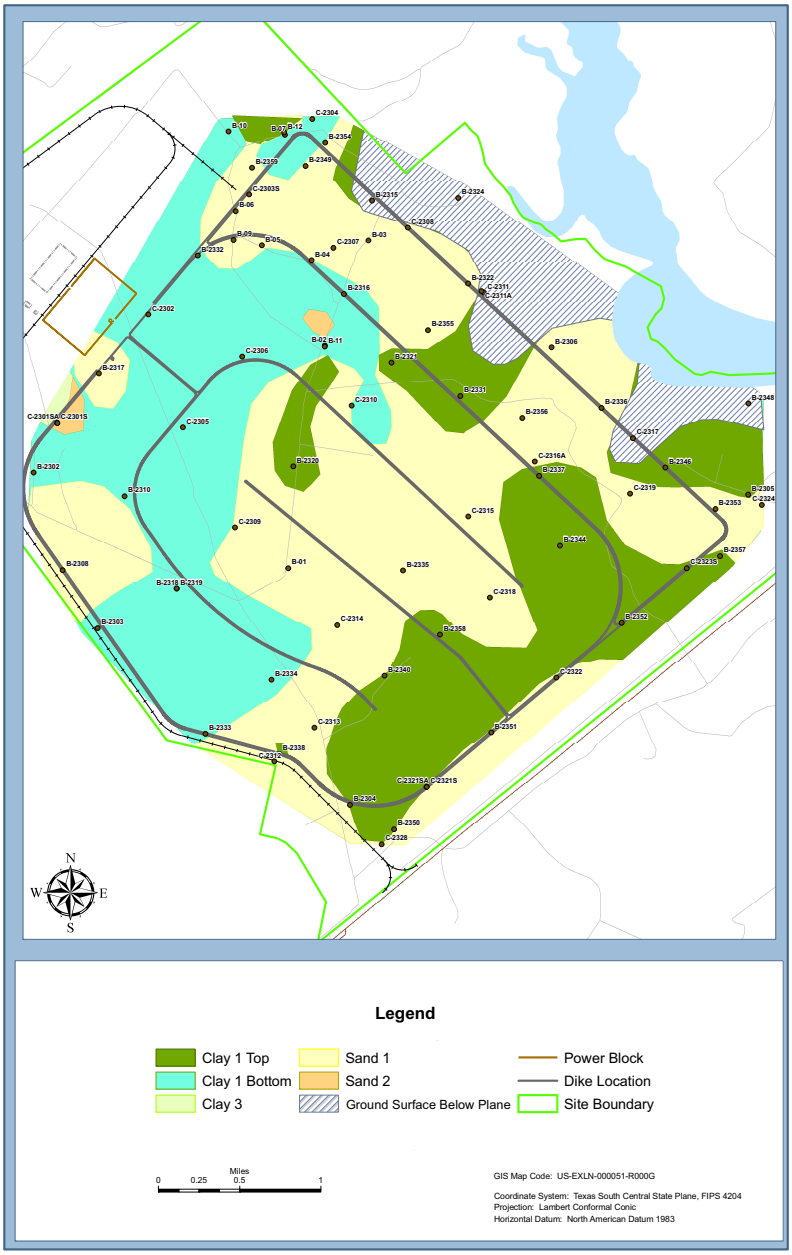

Figure 2.5.5-206 Subsurface Stratigraphy; Elevation 55 Feet (NAVD 88)

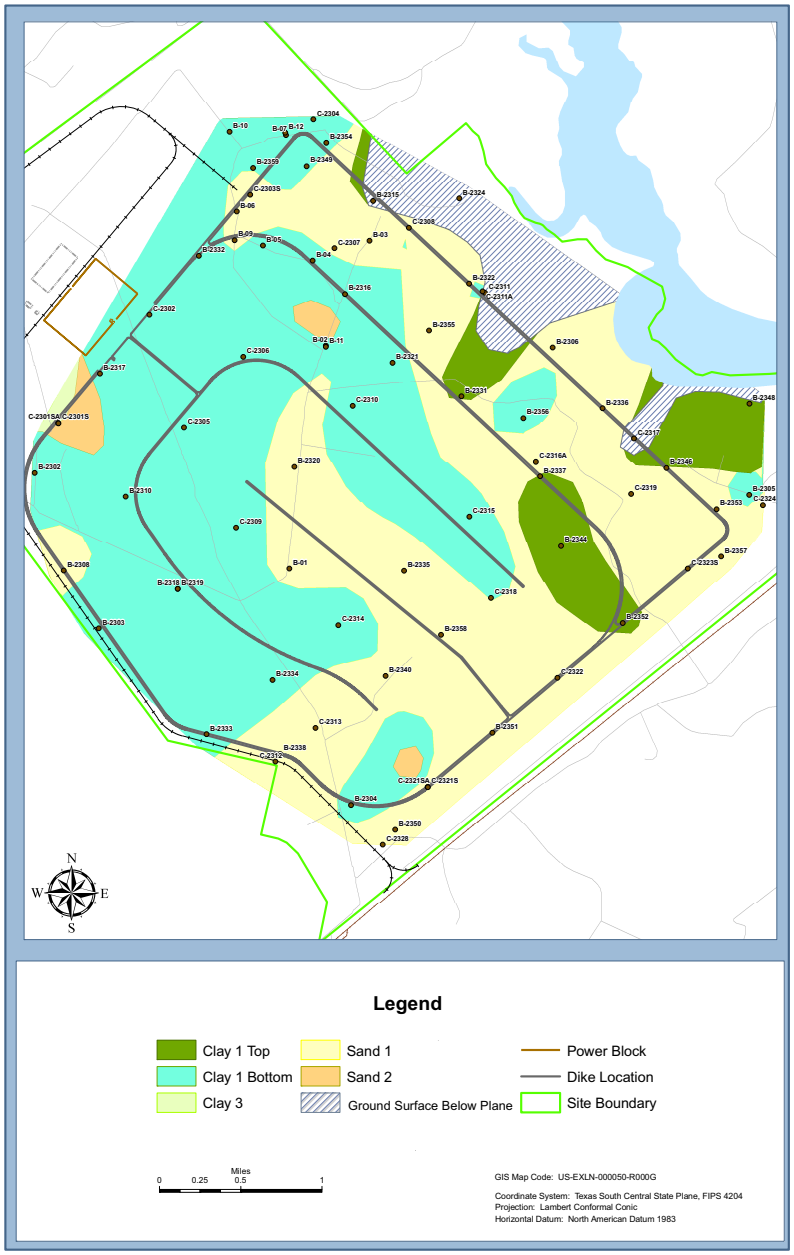

Figure 2.5.5-207 Subsurface Stratigraphy; Elevation 50 Feet (NAVD 88)

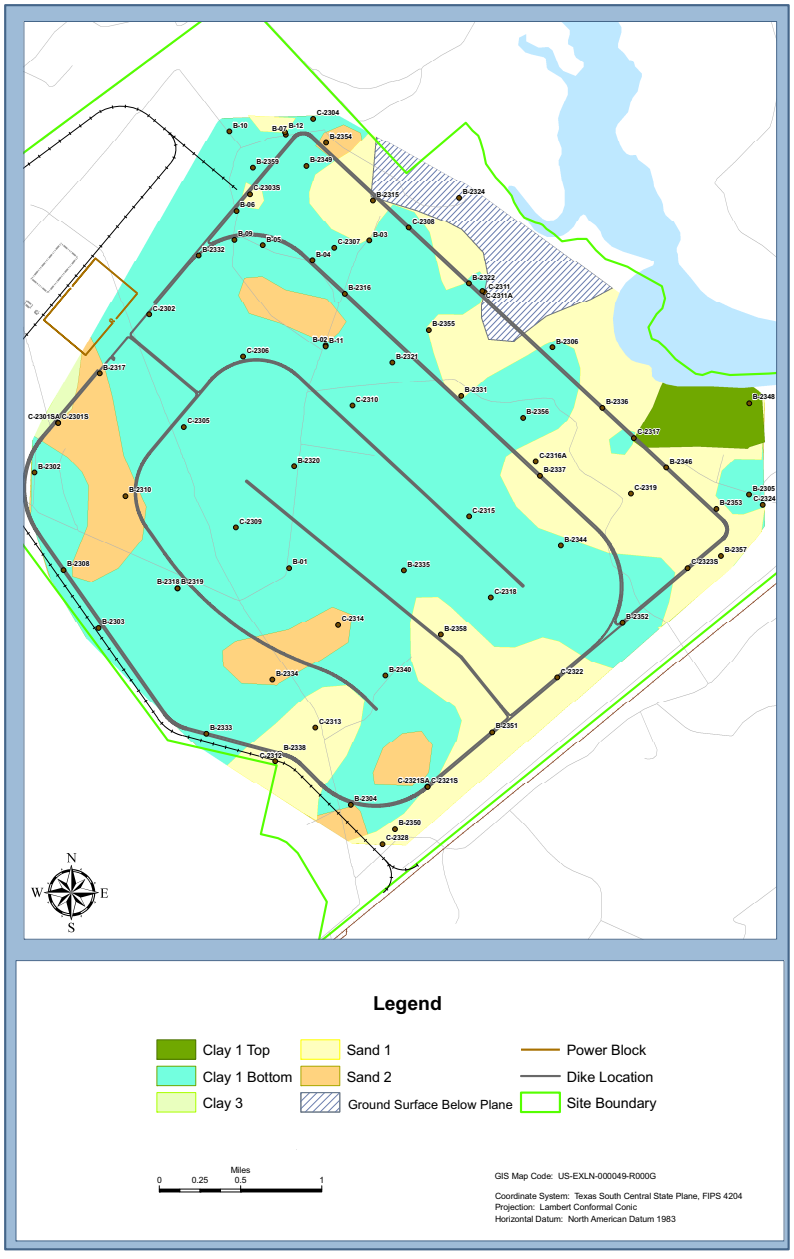

Figure 2.5.5-208 Subsurface Stratigraphy; Elevation 45 Feet (NAVD 88)

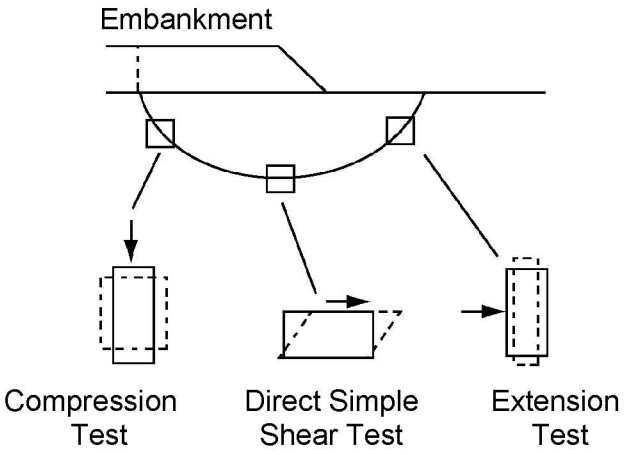

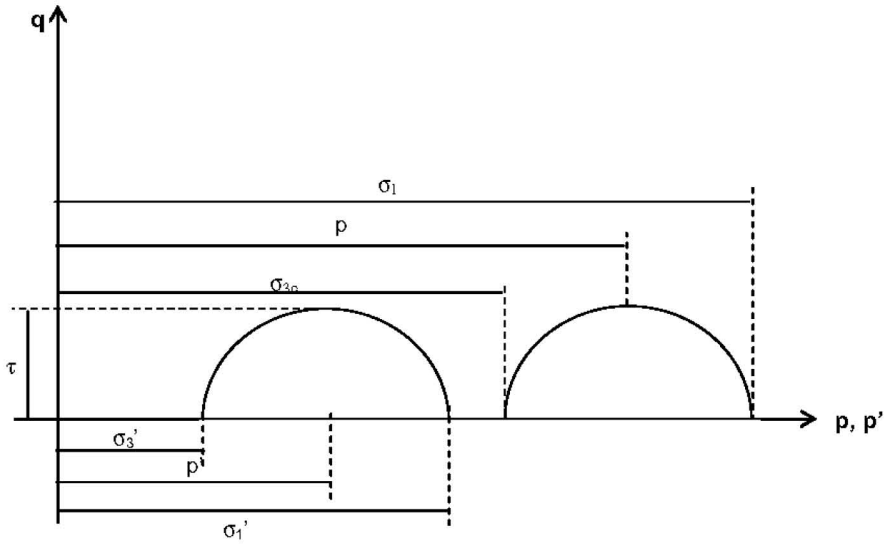

$$\tau = \frac{\sigma_1 - \sigma_3}{2} = \frac{\sigma_1' - \sigma_3'}{2} = q$$

$$p = \frac{\sigma_1 + \sigma_{3c}}{2} = q + \sigma_{3c}$$

$$p' = \frac{\sigma_1' + \sigma_3'}{2} = q + \sigma_3'$$

Figure 2.5.5-209 Applicability of Laboratory Tests to Slope Stability Analysis

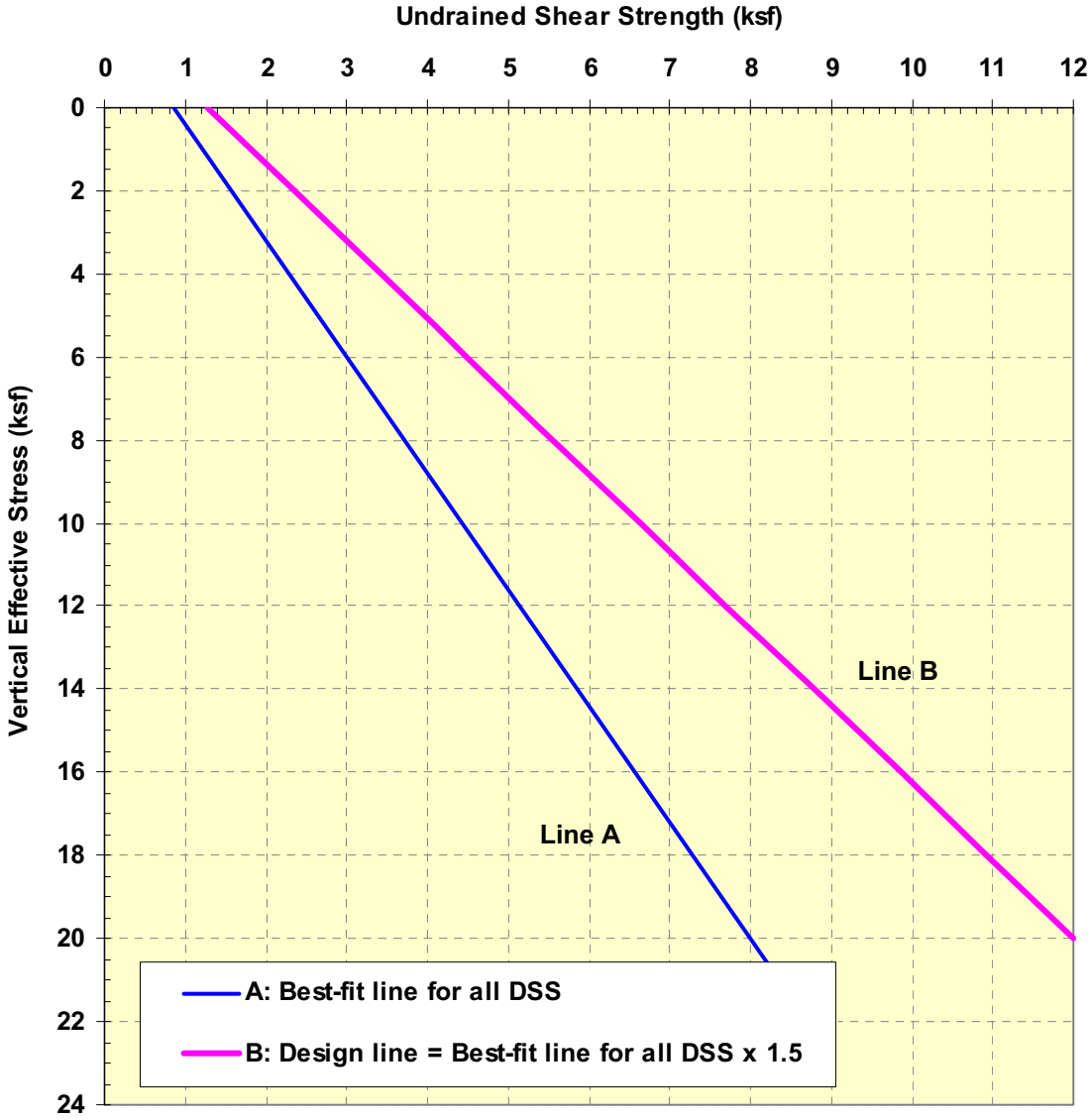

Figure 2.5.5-210 Undrained Shear Strength of Embankment Fill (Composite "A"/Sand and Composite "B"/Clay) Under Plane Strain Conditions

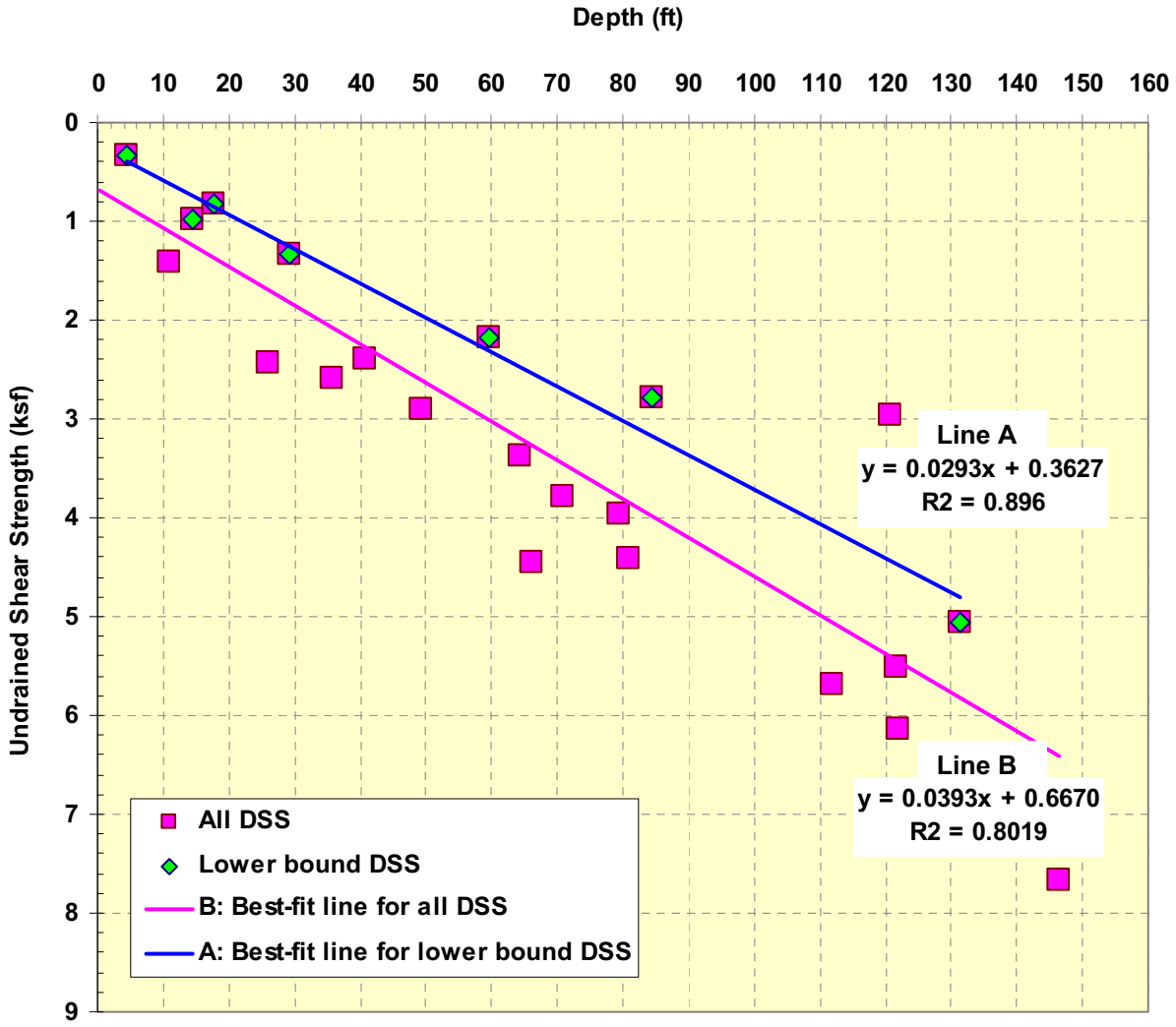

Figure 2.5.5-211 Variation with Depth of the Undrained Shear Strenth of Foundation Clays

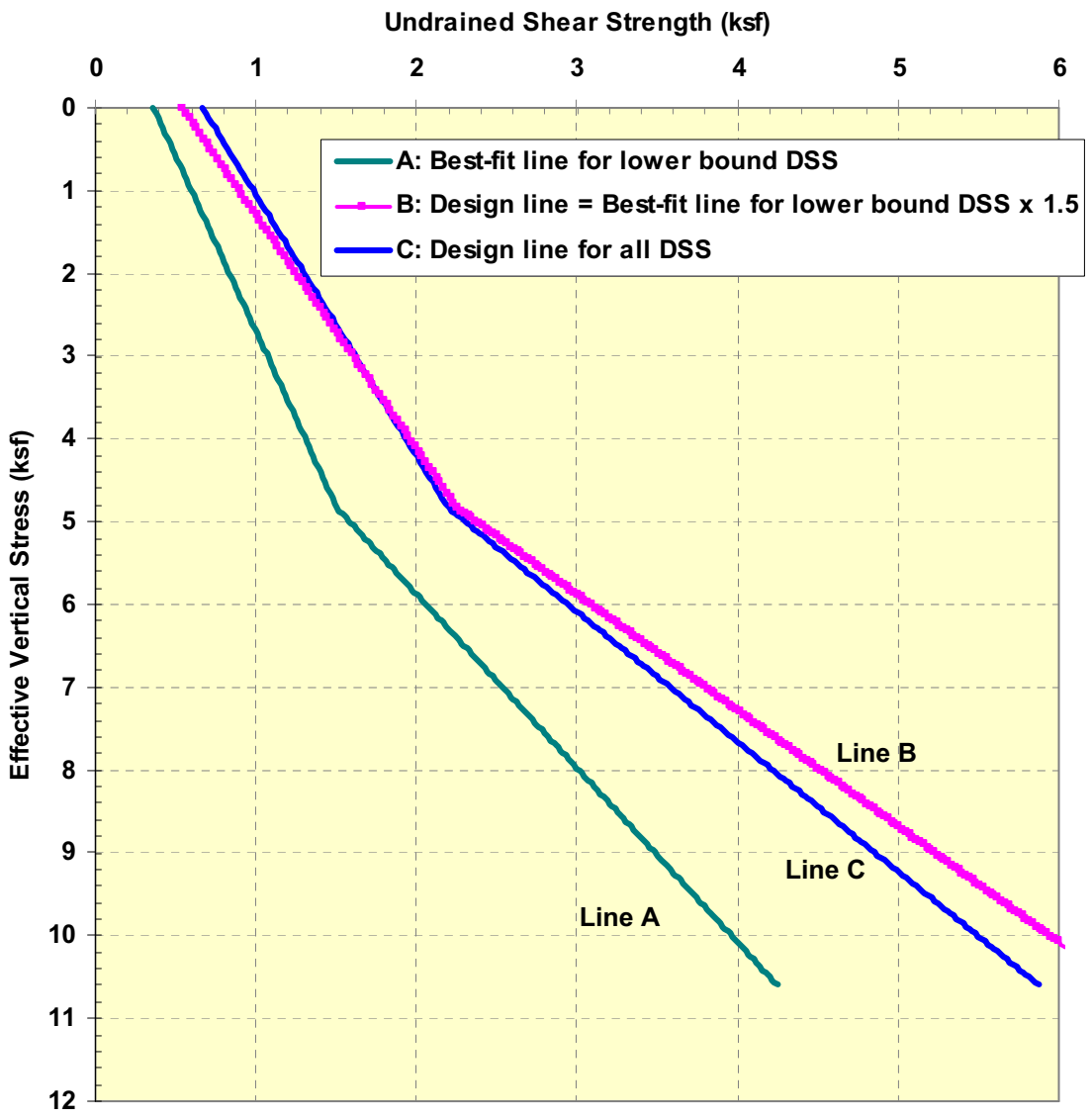

Effective vertical stresses are calculated based on the following: average ground surface at elevation 72.5 feet (NAVD 88), average groundwater level at elevation 33.5 feet (NAVD 88), and average total unit weight at 124 pcf.

Figure 2.5.5-212 Undrained Shear Strength of Foundation Clays Under Simple Shear Conditions

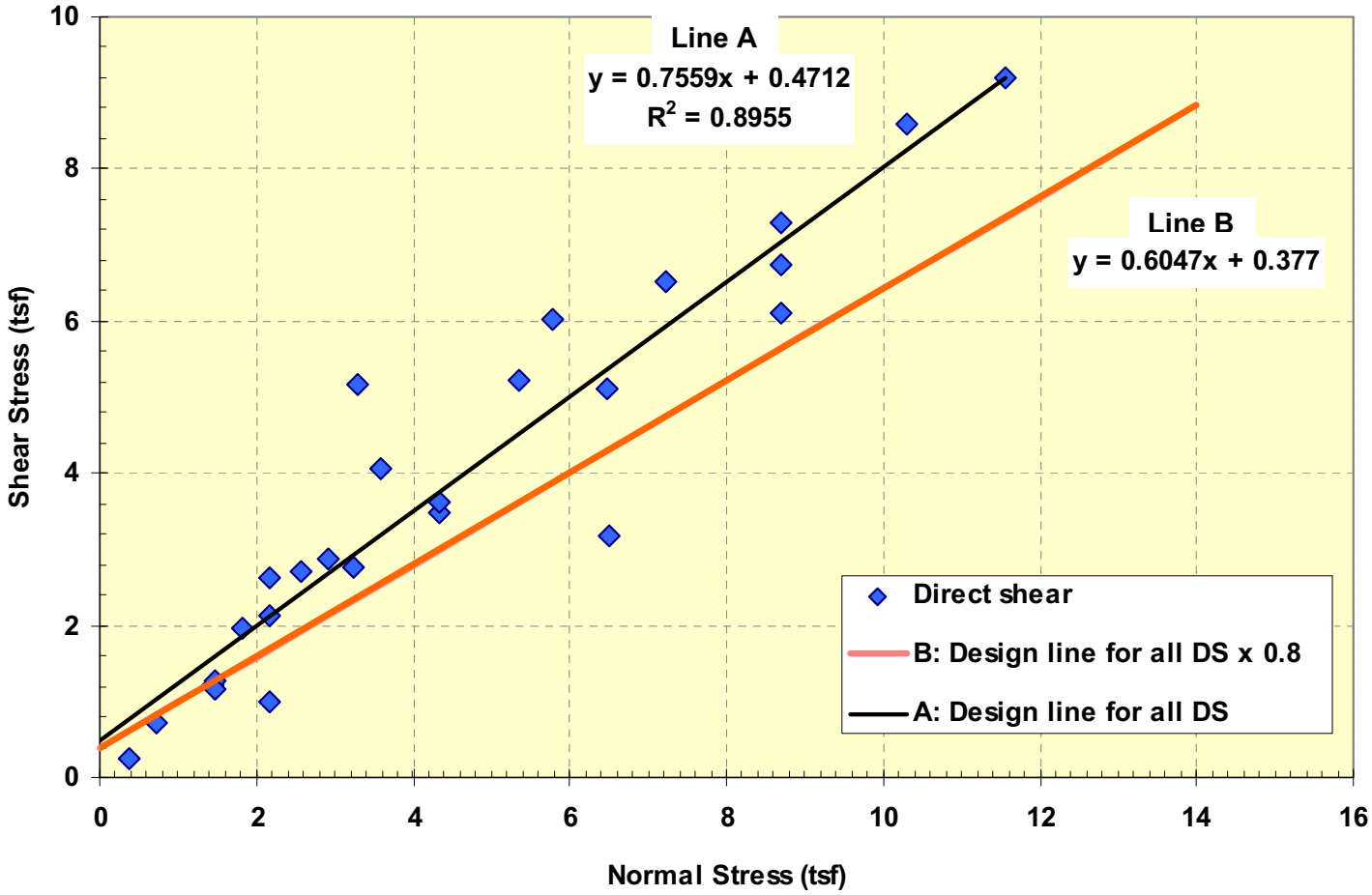

Notes:
Test values x 80% are used in the post-earthquake stability analysis, i.e., line B.
Plane strain correction is not applied to either line.

Figure 2.5.5-213 Effective Strength Parameters of Foundation Sands Derived from Direct Shear Tests

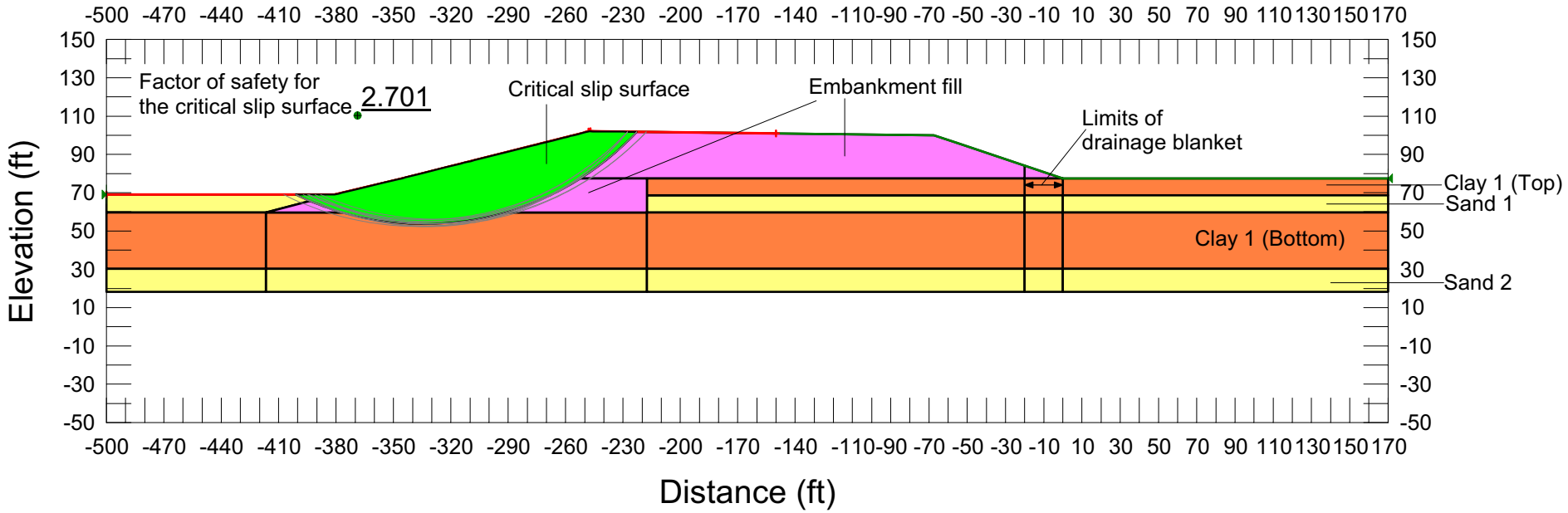

Notes:
Horizontal lines represent subsurface stratification and embankment fill limits
Vertical lines represent different region generation
Factor of safety is shown at a convenient location on the figure; does not represent the actual center point of the slip circle

Figure 2.5.5-214 Slope Stability; Shortly After Construction Case; North Dam of Cooling Basin at Cone Penetration Test C-2302

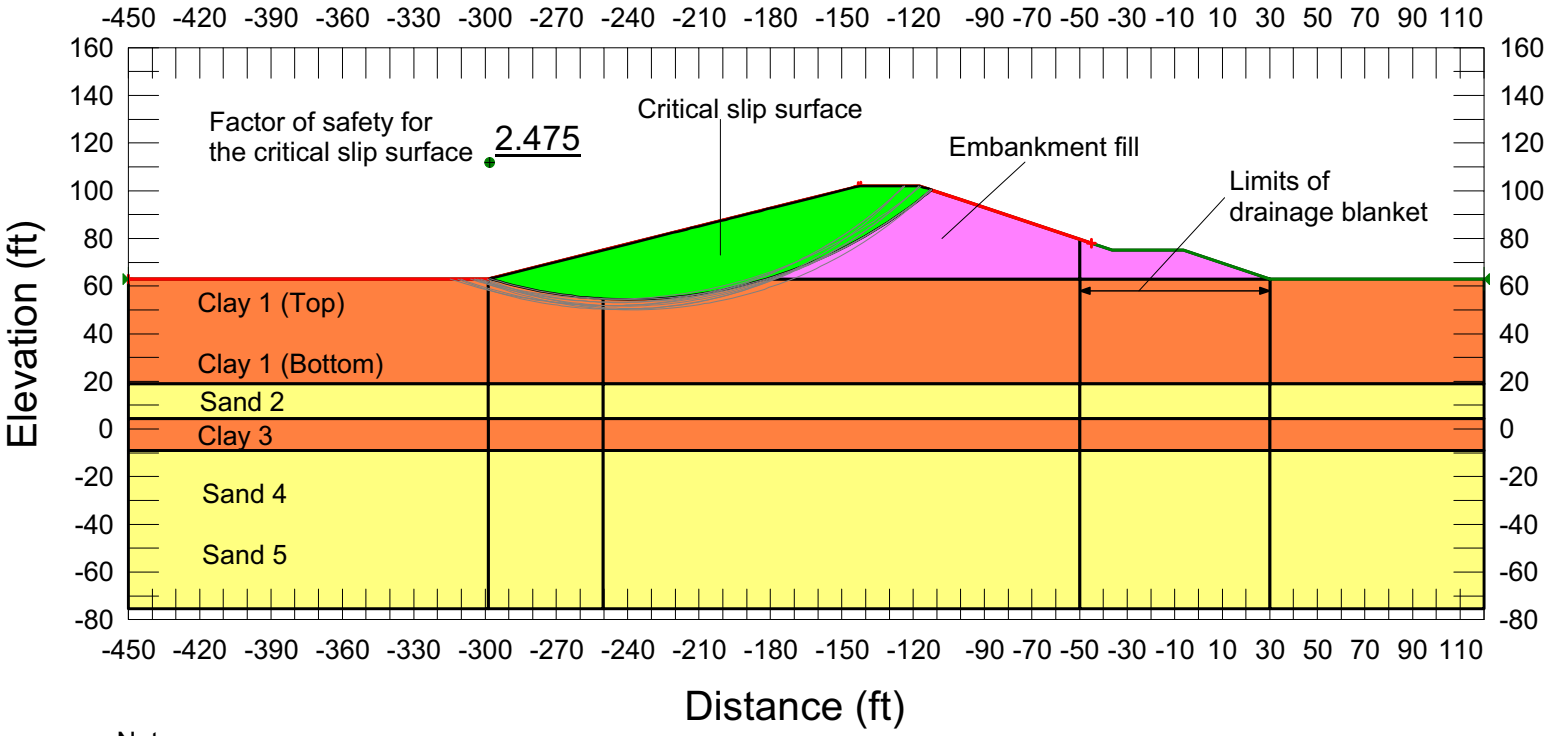

Notes:
Horizontal lines represent subsurface stratification and embankment fill limits
Vertical lines represent different region generation
Factor of safety is shown at a convenient location on the figure; does not represent the actual center point of the slip surface

Figure 2.5.5-215 Slope Stability; Shortly After Construction Case; South Dam of Cooling Basin at Boring B-2352

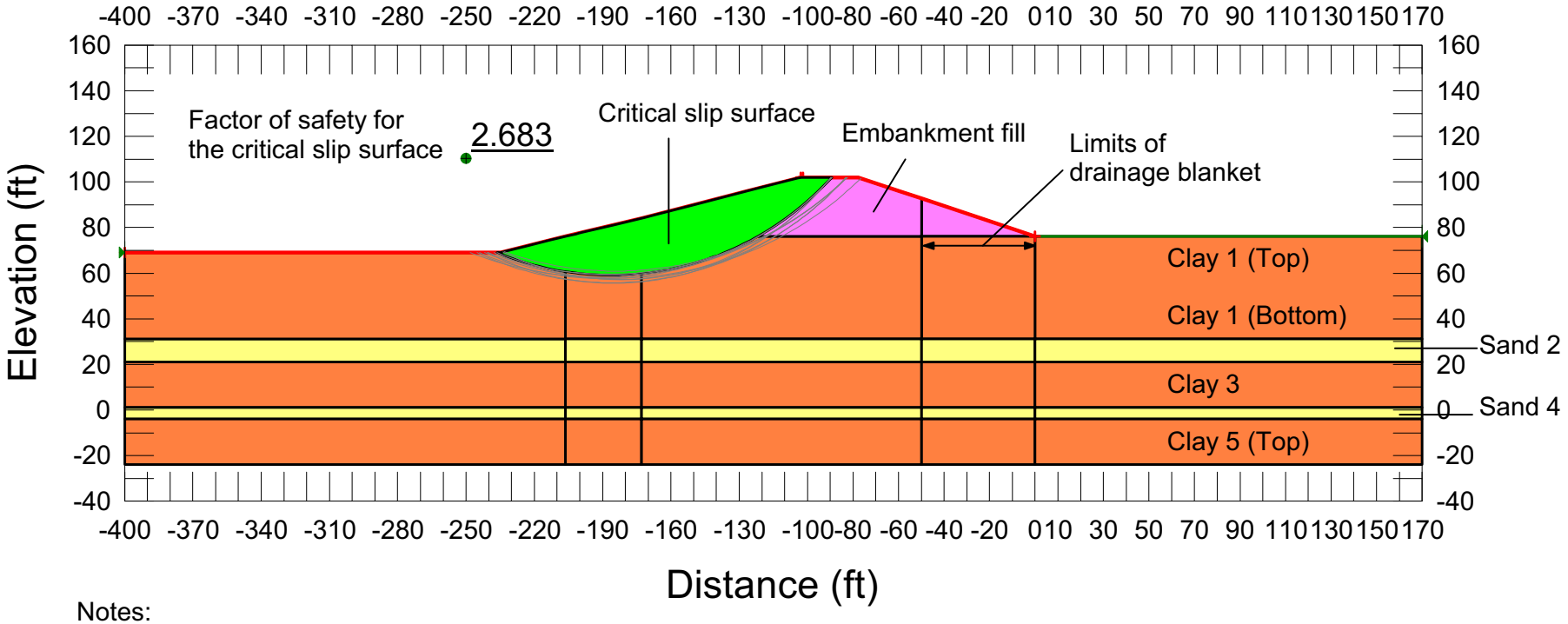

Notes:
Horizontal lines represent subsurface stratification and embankment fill limits
Vertical lines represent different region generation
Factor of safety is shown at a convenient location on the figure; does not represent the actual center point of the slip circle

Figure 2.5.5-216 Slope Stability; Shortly After Construction Case; West Dam of Cooling Basin at Boring B-2333

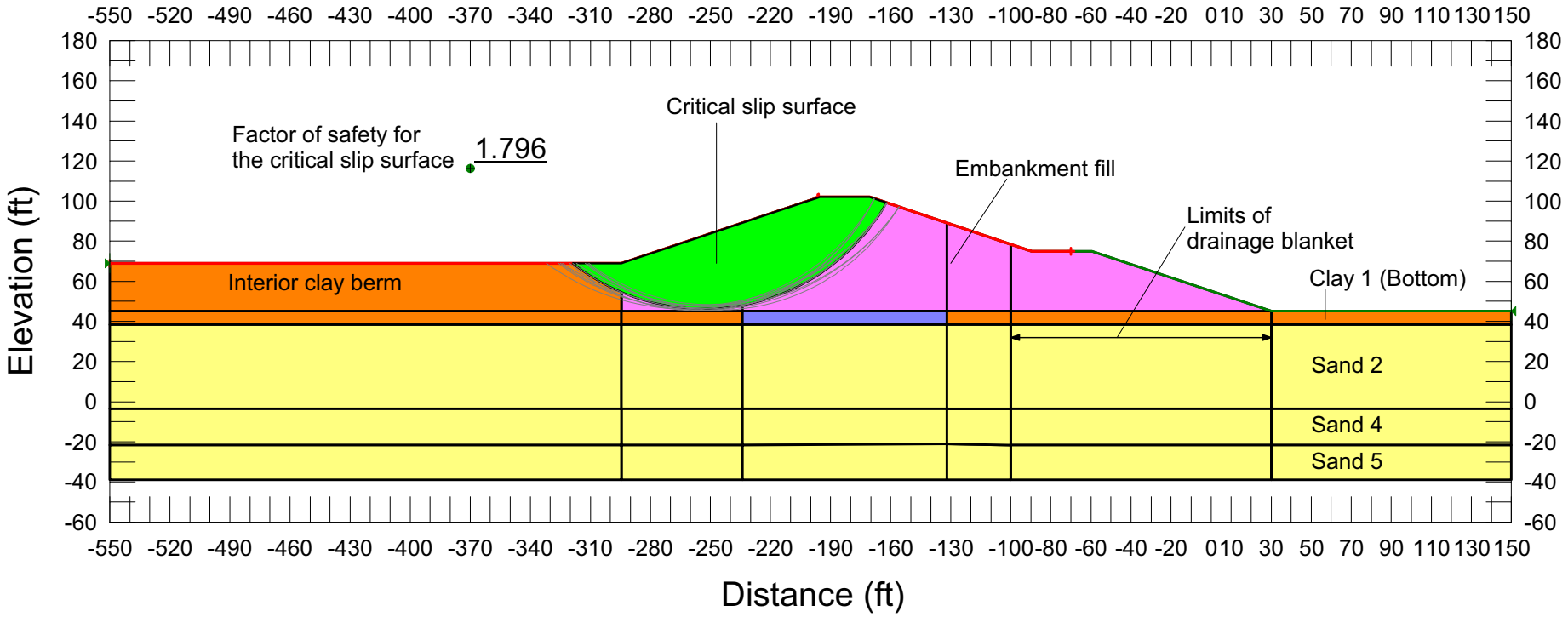

Notes:
Horizontal lines represent subsurface stratification and embankment fill limits
Vertical lines represent different region generation
Factor of safety is shown at a convenient location on the figure; does not represent the actual center point of the slip circle

Figure 2.5.5-217 Slope Stability; Shortly After Construction Case; East Dam of GBRA Storage Water Reservoir at Cone Penetration Test C-2317

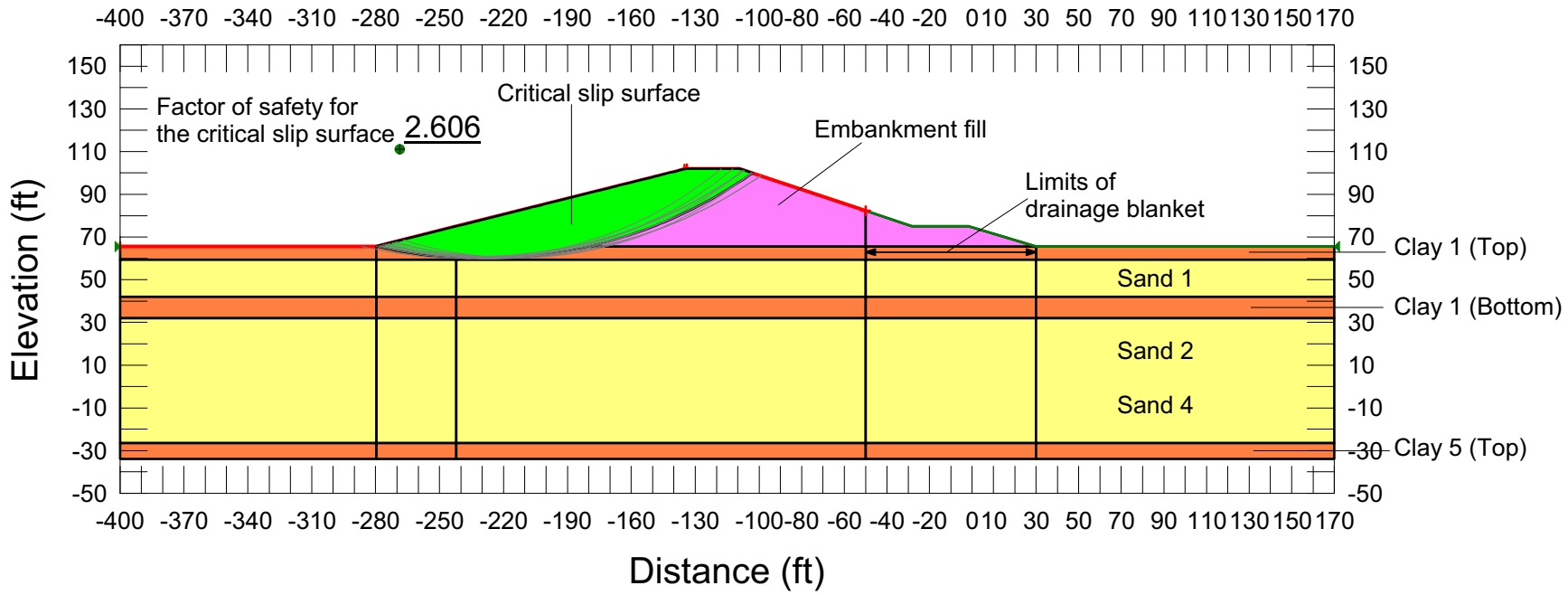

Notes:
Horizontal lines represent subsurface stratification and embankment fill limits
Vertical lines represent different region generation
Factor of safety is shown at a convenient location on the figure; does not represent the actual center point of the slip circle

Figure 2.5.5-218 Slope Stability; Shortly After Construction Case; East Dam of GBRA Storage Water Reservoir at Boring B-2353

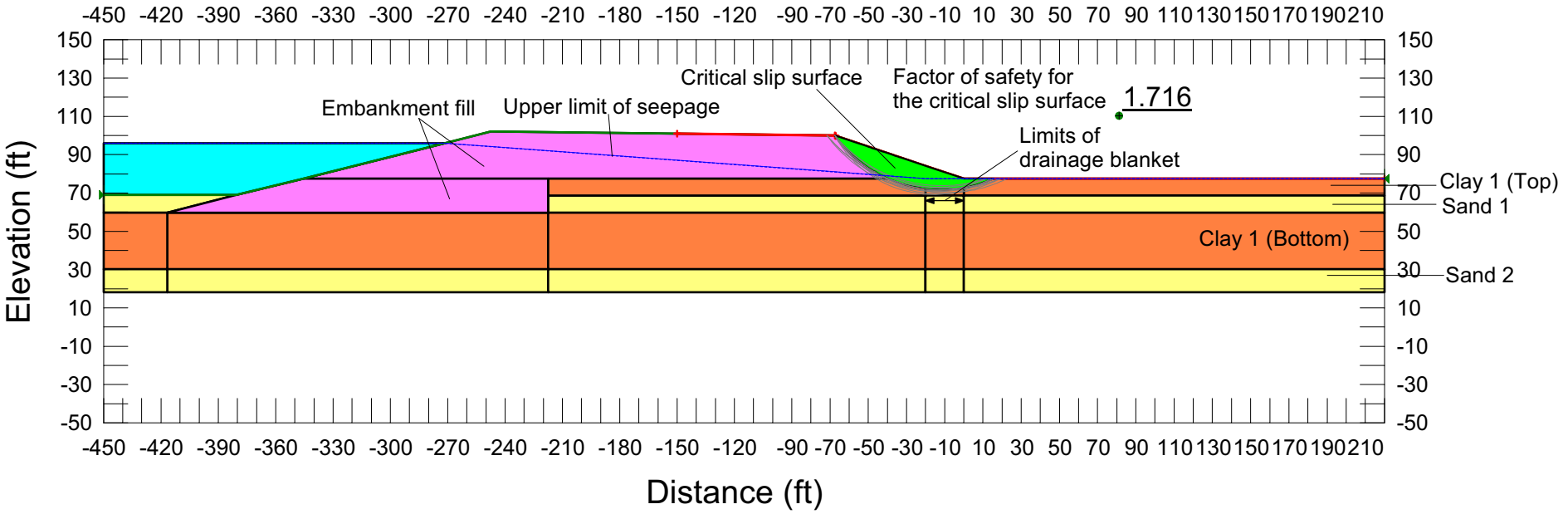

Notes:
Horizontal lines represent subsurface stratification and embankment fill limits
Vertical lines represent different region generation
Factor of safety is shown at a convenient location on the figure; does not represent the actual center point of the slip circle

Figure 2.5.5-219 Slope Stability; Steady-State Seepage Case; North Dam of Cooling Basin at Cone Penetration Test C-2302

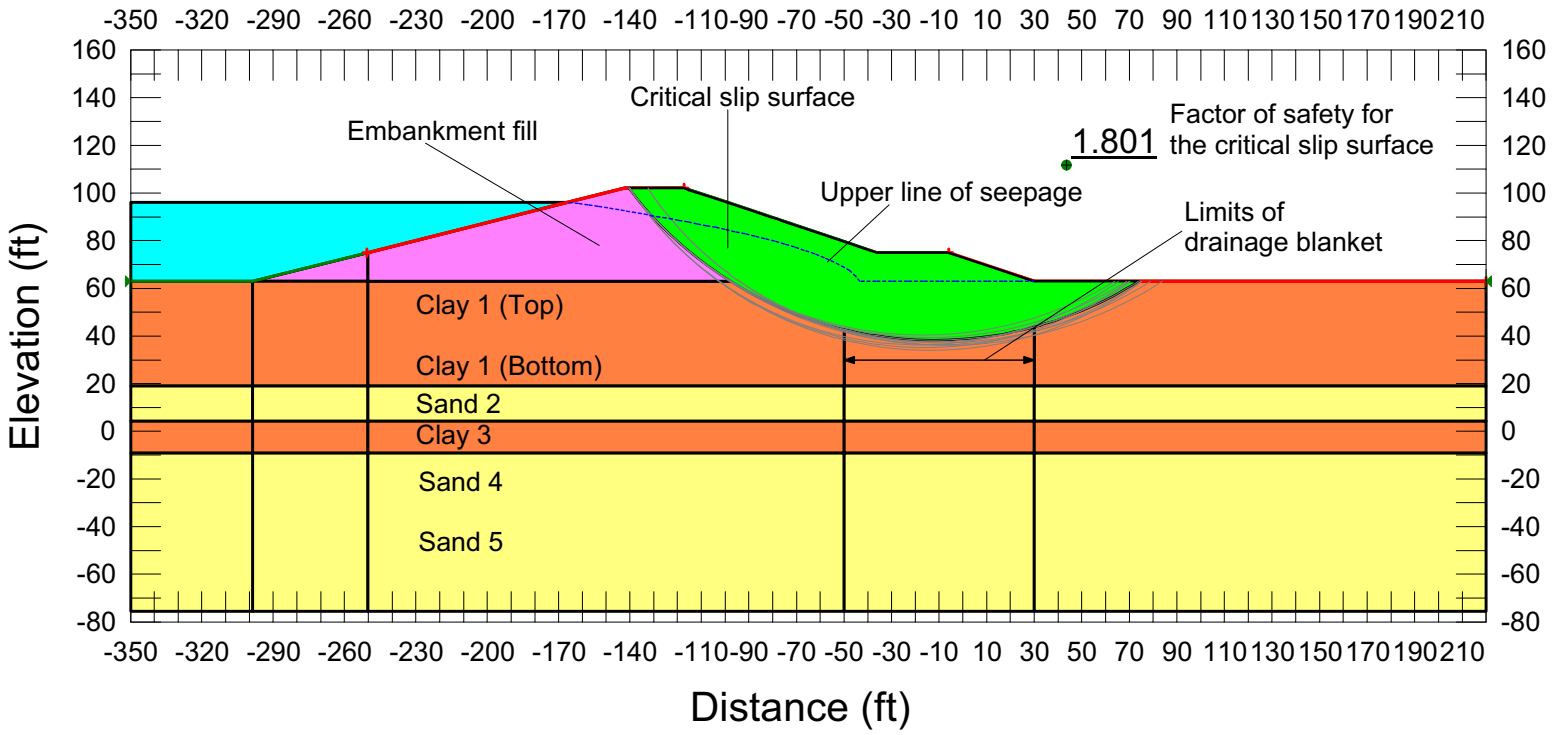

Notes:
Horizontal lines represent subsurface stratification and embankment fill limits
Vertical lines represent different region generation
Factor of safety is shown at a convenient location on the figure; does not represent the actual center point of the slip circle

Figure 2.5.5-220 Slope Stability; Steady-State Seepage Case; South Dam of Cooling Basin at Boring B-2352

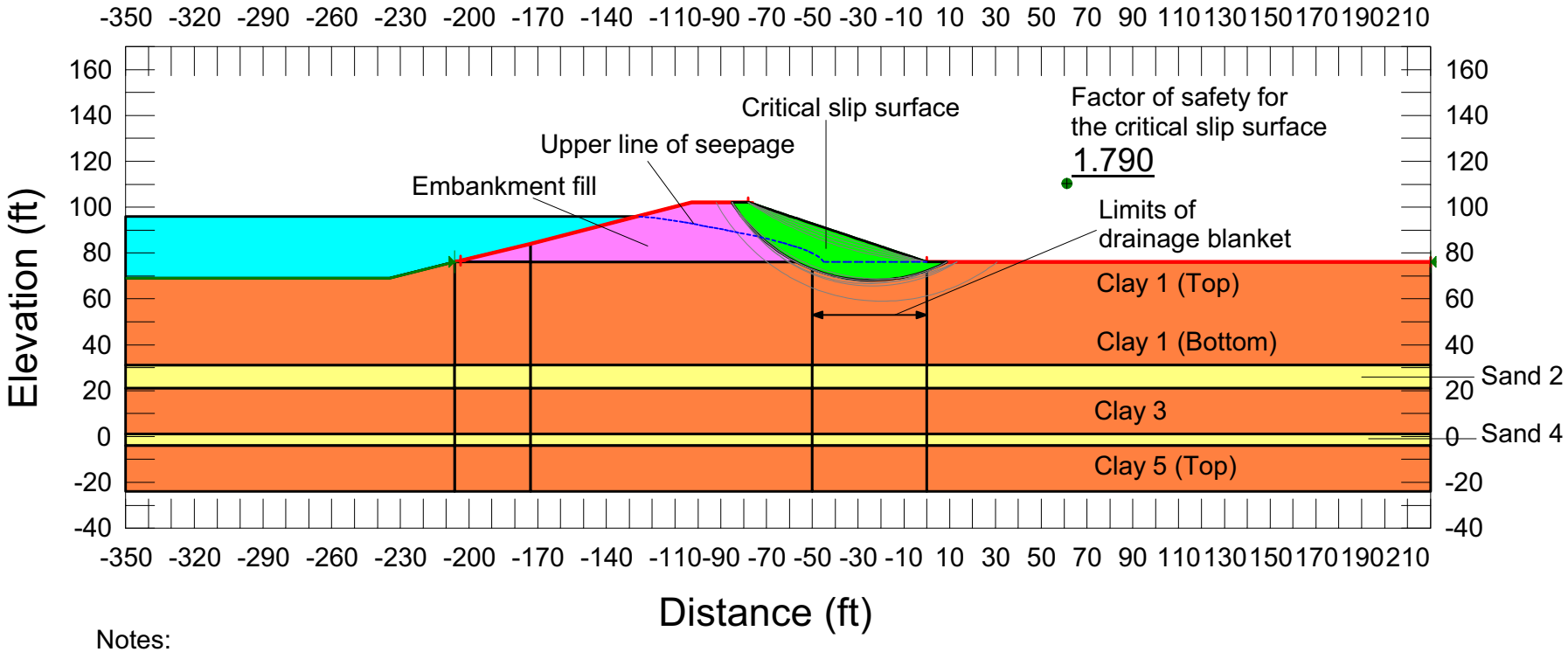

Notes:
Horizontal lines represent subsurface stratification and embankment fill limits
Vertical lines represent different region generation
Factor of safety is shown at a convenient location on the figure; does not represent the actual center point of the slip circle

Figure 2.5.5-221 Slope Stability; Steady-State Seepage Case; West Dam of Cooling Basin at Boring B-2333

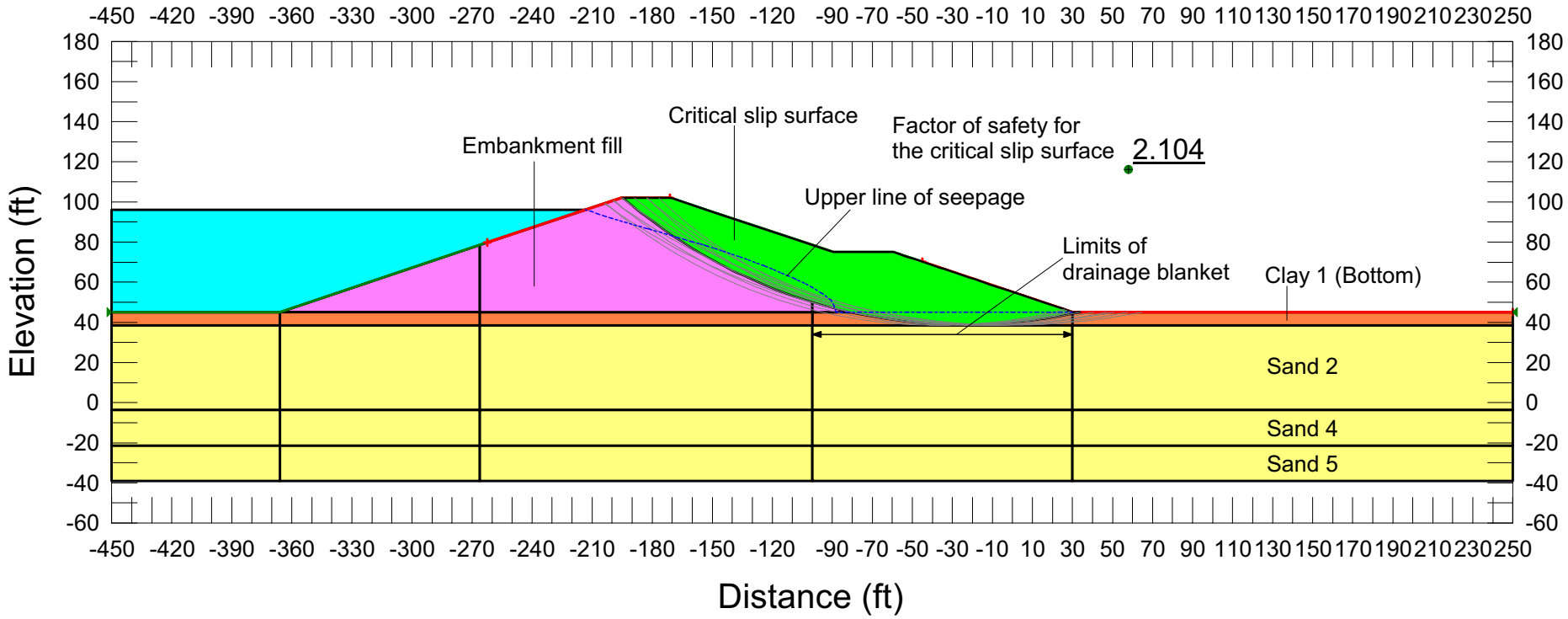

Notes:
Horizontal lines represent subsurface stratification and embankment fill limits
Vertical lines represent different region generation
Factor of safety is shown at a convenient location on the figure; does not represent the actual center point of the slip circle

Figure 2.5.5-222 Slope Stability; Steady-State Seepage Case; East Dam of GBRA Storaeg Water Reservoir at Cone Penetration Test C-2317

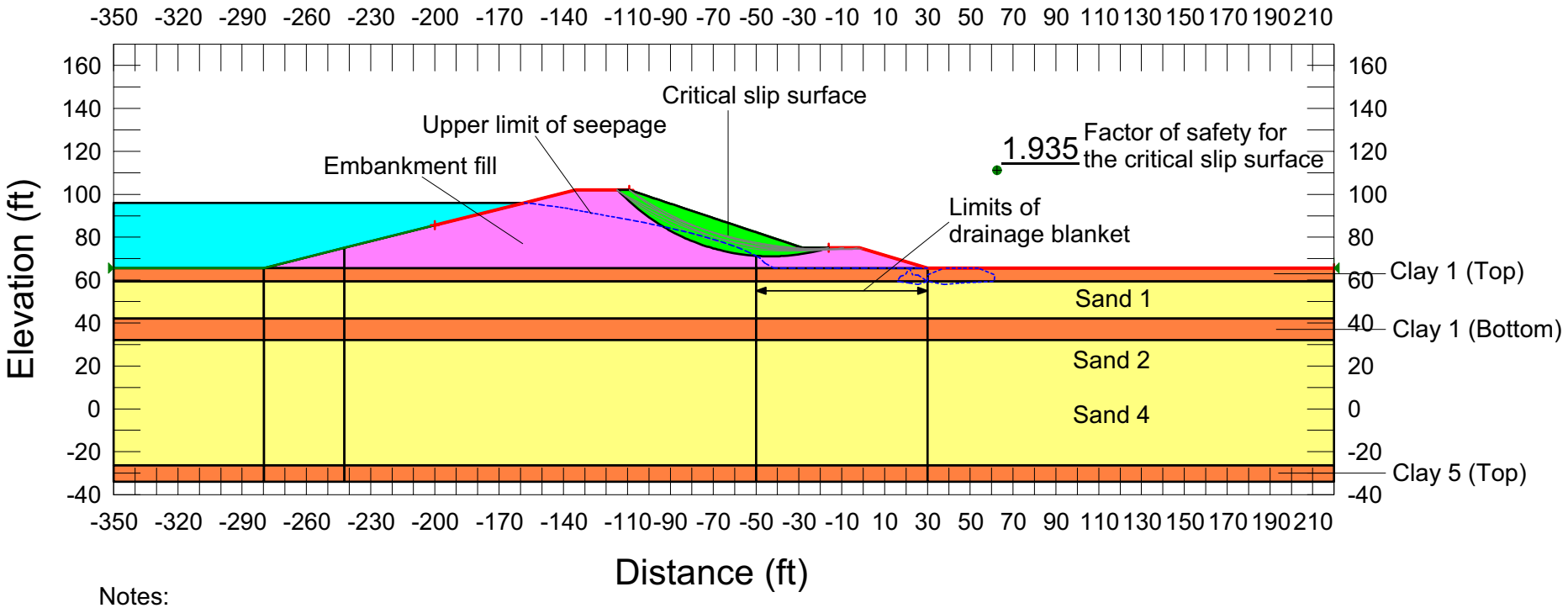

Notes:
Horizontal lines represent subsurface stratification and embankment fill limits
Vertical lines represent different region generation
Factor of safety is shown at a convenient location on the figure; does not represent the actual center point of the slip circle

Figure 2.5.5-223 Slope Stability; Steady-State Seepage Case; East Dam of GBRA Storage Water Reservoir at Boring B-2353

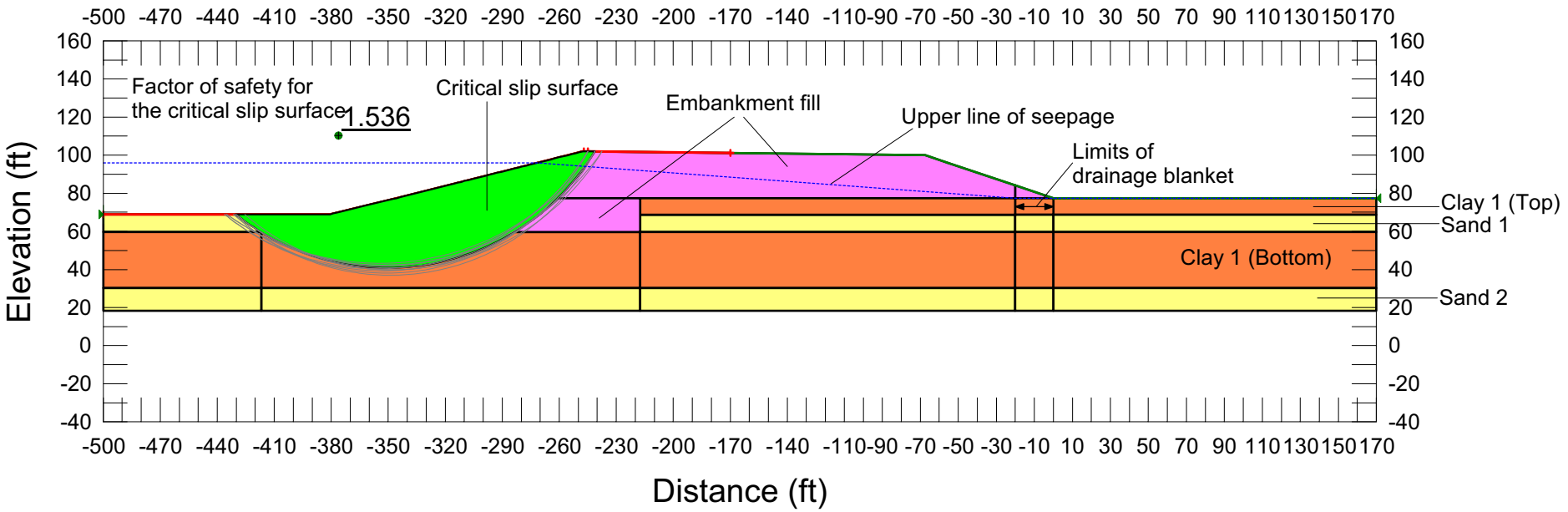

Notes:
Horizontal lines represent subsurface stratifiation and embankment fill limits
Vertical lines represent different region generation
Factor of safety is shown at a convenient location on the figure; does not represent the actual center point of the slip circle

Figure 2.5.5-224 Slope Stability; Rapid Drawdown Case; North Dam of Cooling Basin at Cone Penetration Test C-2302

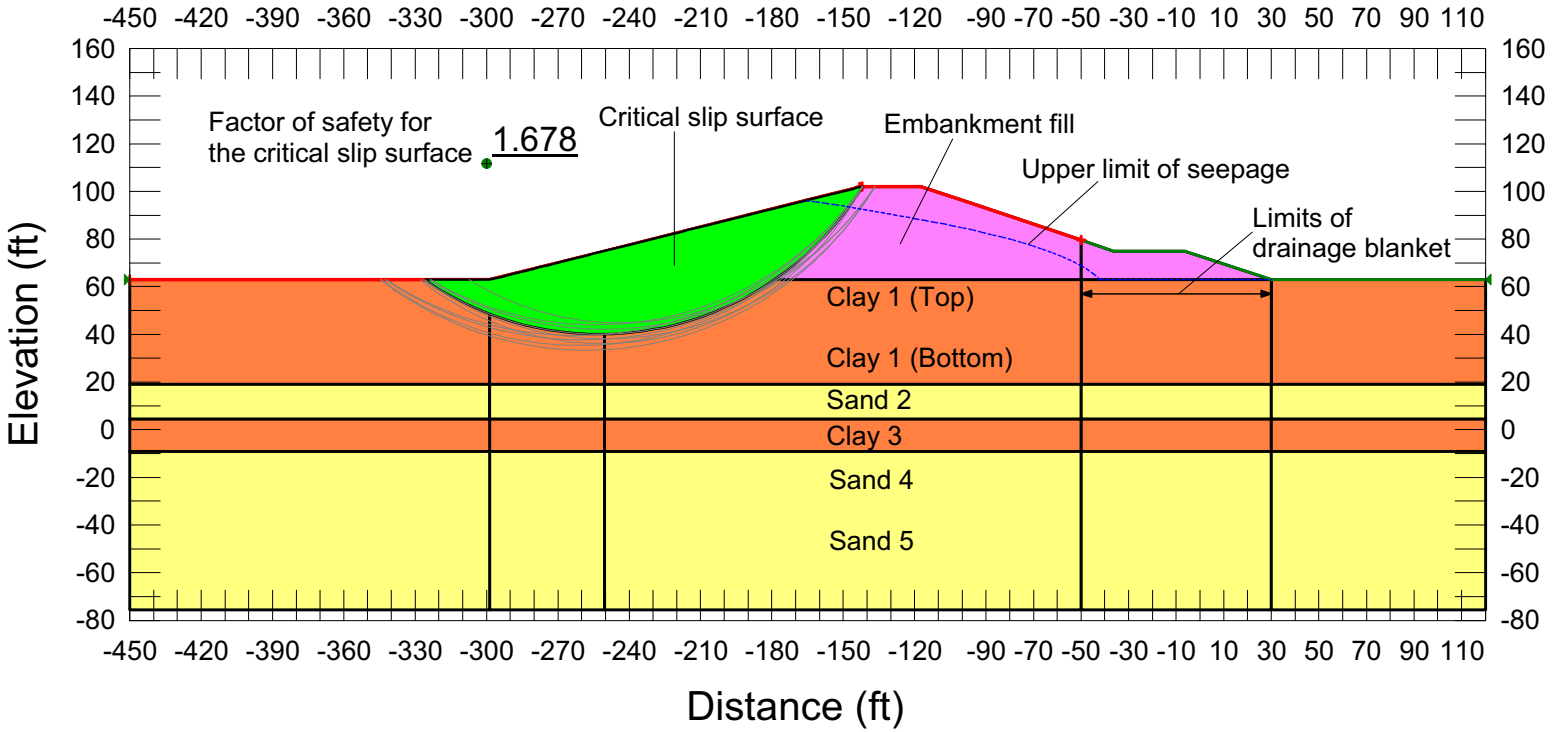

Notes:
Horizontal lines represent subsurface stratification and embankment fill limits
Vertical lines represent different region generation
Factor of safety is shown at a convenient location on the figure; does not represent the actual center point of the slip circle

Figure 2.5.5-225 Slope Stability; Rapid Drawdown Case; South Dam of Cooling Basin at Boring B-2352

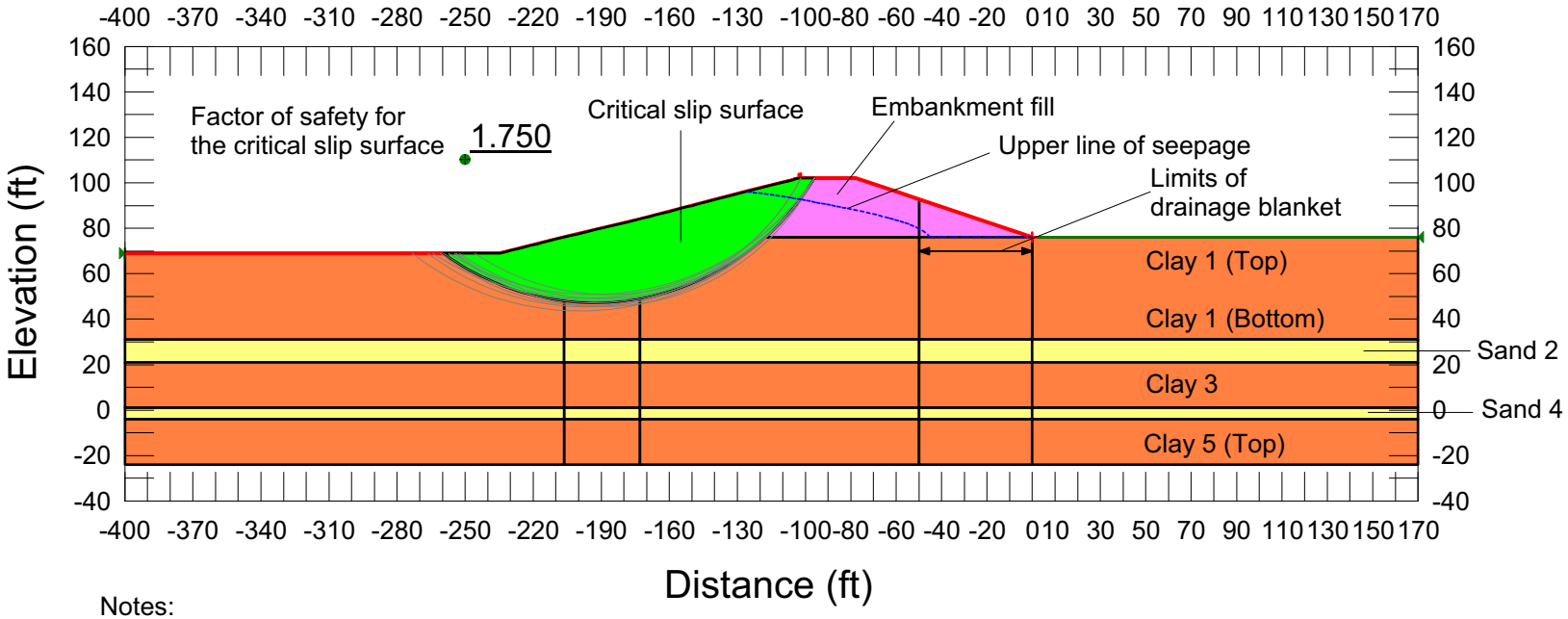

Notes:
Horizontal lines represent subsurface stratification and embankment fill limits
Vertical lines represent different region generation
Factor of safety is shown at a convenient location on the figure; does not represent the actual center point of the slip circle

Figure 2.5.5-226 Slope Stability; Rapid Drawdown Case; West Dam of Cooling Basin at Boring B-2333

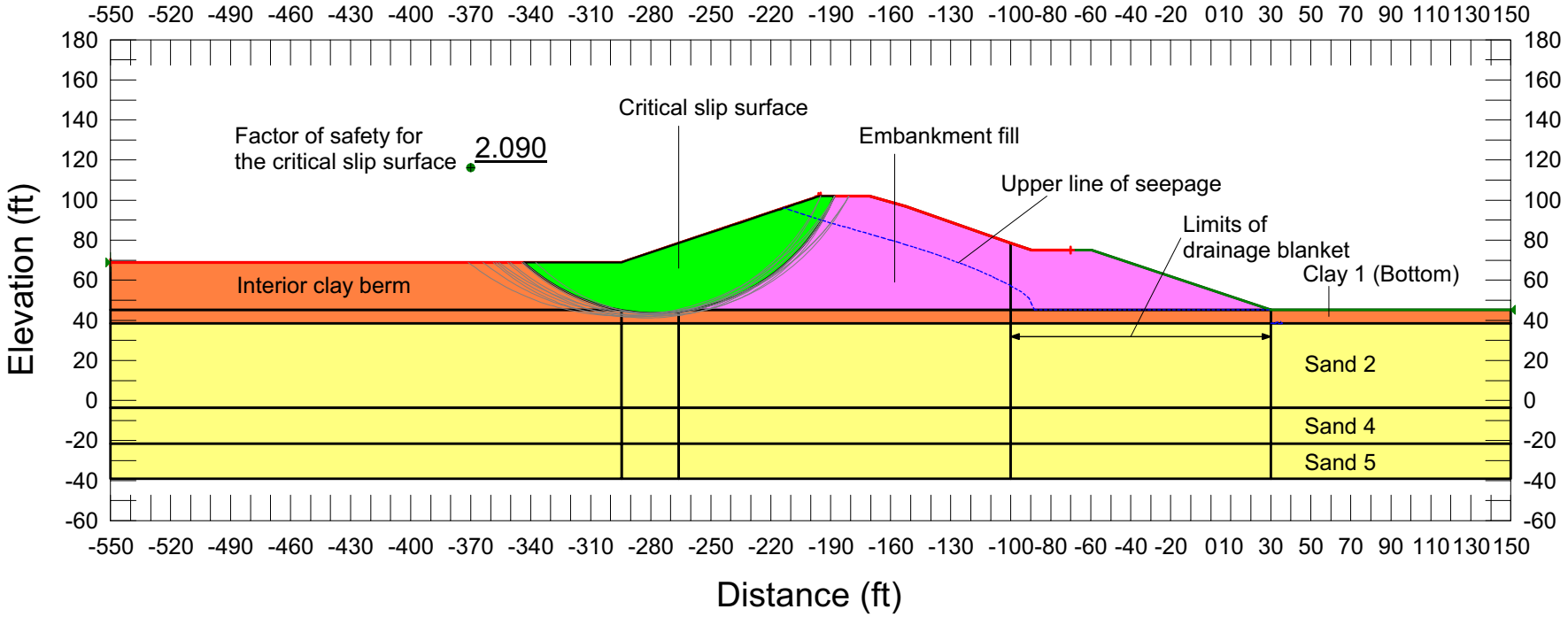

Notes:
Horizontal lines represent subsurface stratification and embankment fill limits
Vertical lines represent different region generation
Factor of safety is shown at a convenient location on the figure; does not represent the actual center point of the slip circle

**Figure 2.5.5-227 Slope Stability; Rapid Drawdown Case;
East Dam of GBRA Storage Water Reservoir at Cone Penetration Test C-2317**

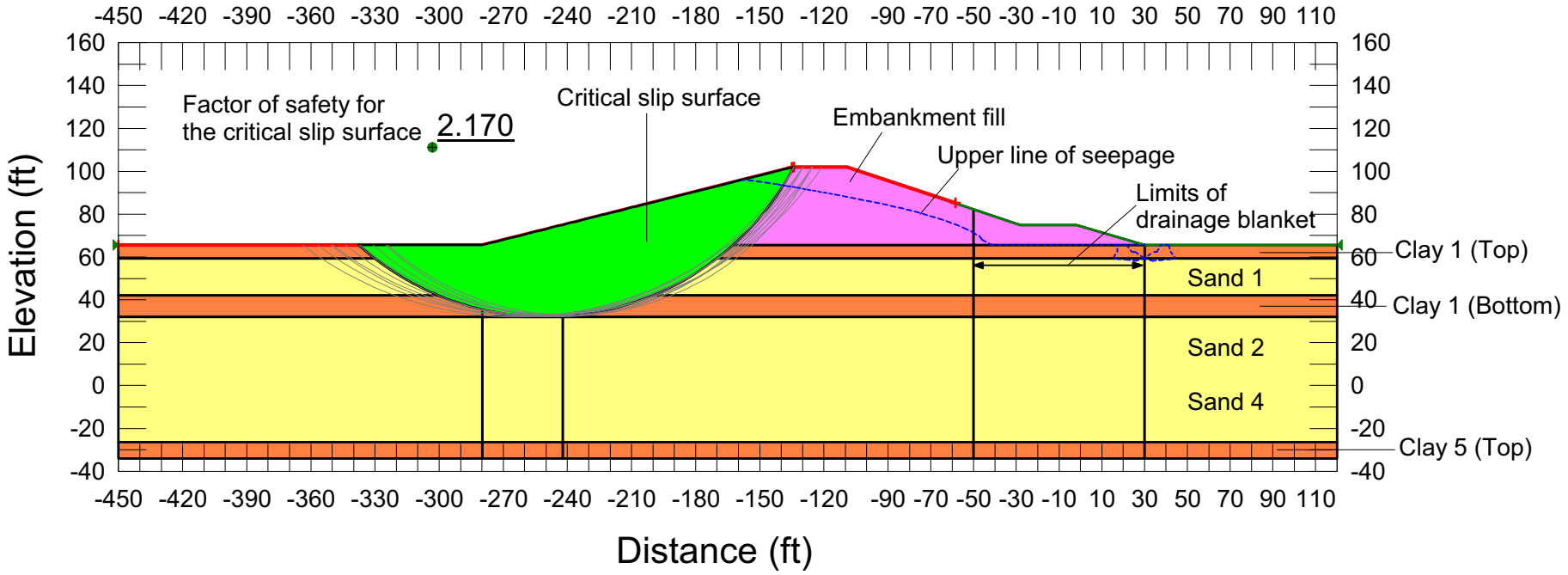

Notes:
Horizontal lines represent subsurface stratification and embankment fill limits
Vertical lines represent different region generation
Factor of safety is shown at a convenient location on the figure; does not represent the actual center point of the slip circle

**Figure 2.5.5-228 Slope Stability; Rapid Drawdown Case;
East Dam of GBRA Storage Water Reservoir at Boring B-2353**

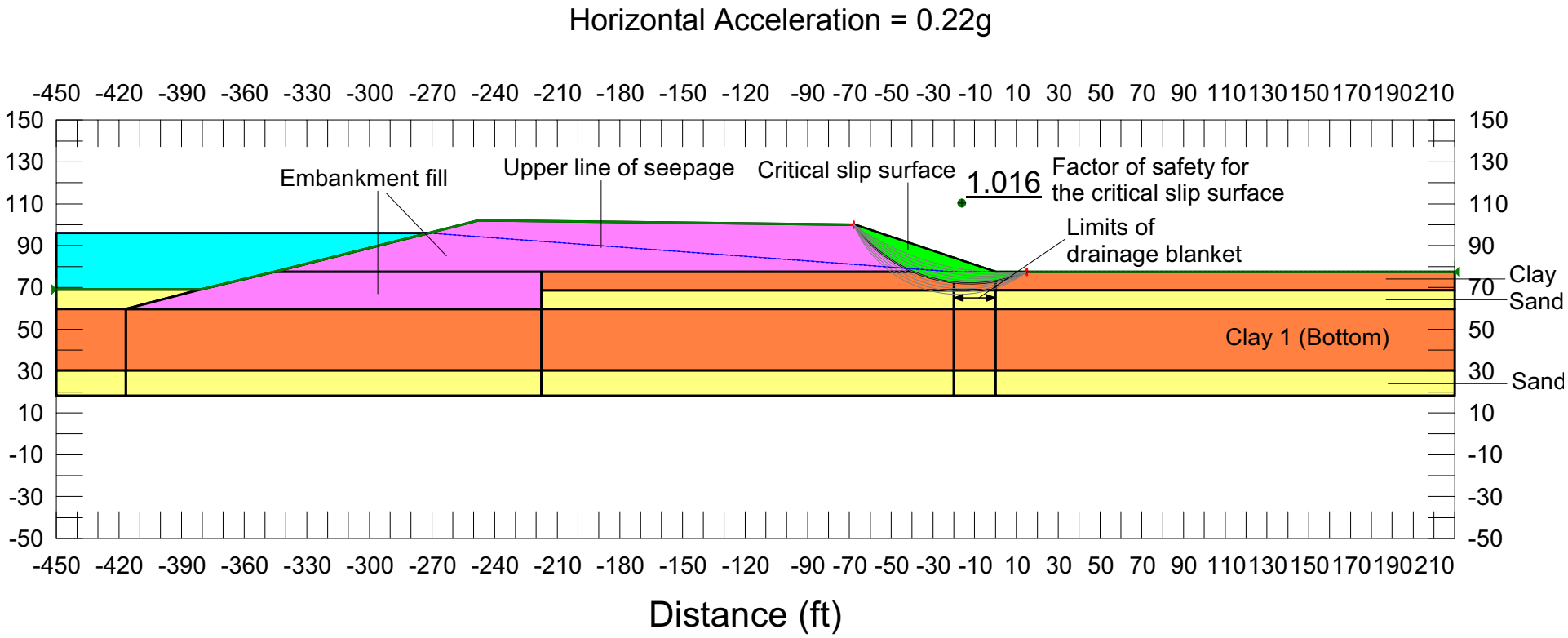

Notes:
Horizontal lines represent subsurface stratification and embankment fill limits
Vertical lines represent different region generation
Factor of safety is shown at a convenient location on the figure; does not represent the actual center point of the slip sircle

Figure 2.5.5-229 Slope Stability; Yield Acceleration; North Dam of Cooling Basin at Cone Penetration Test C-2302

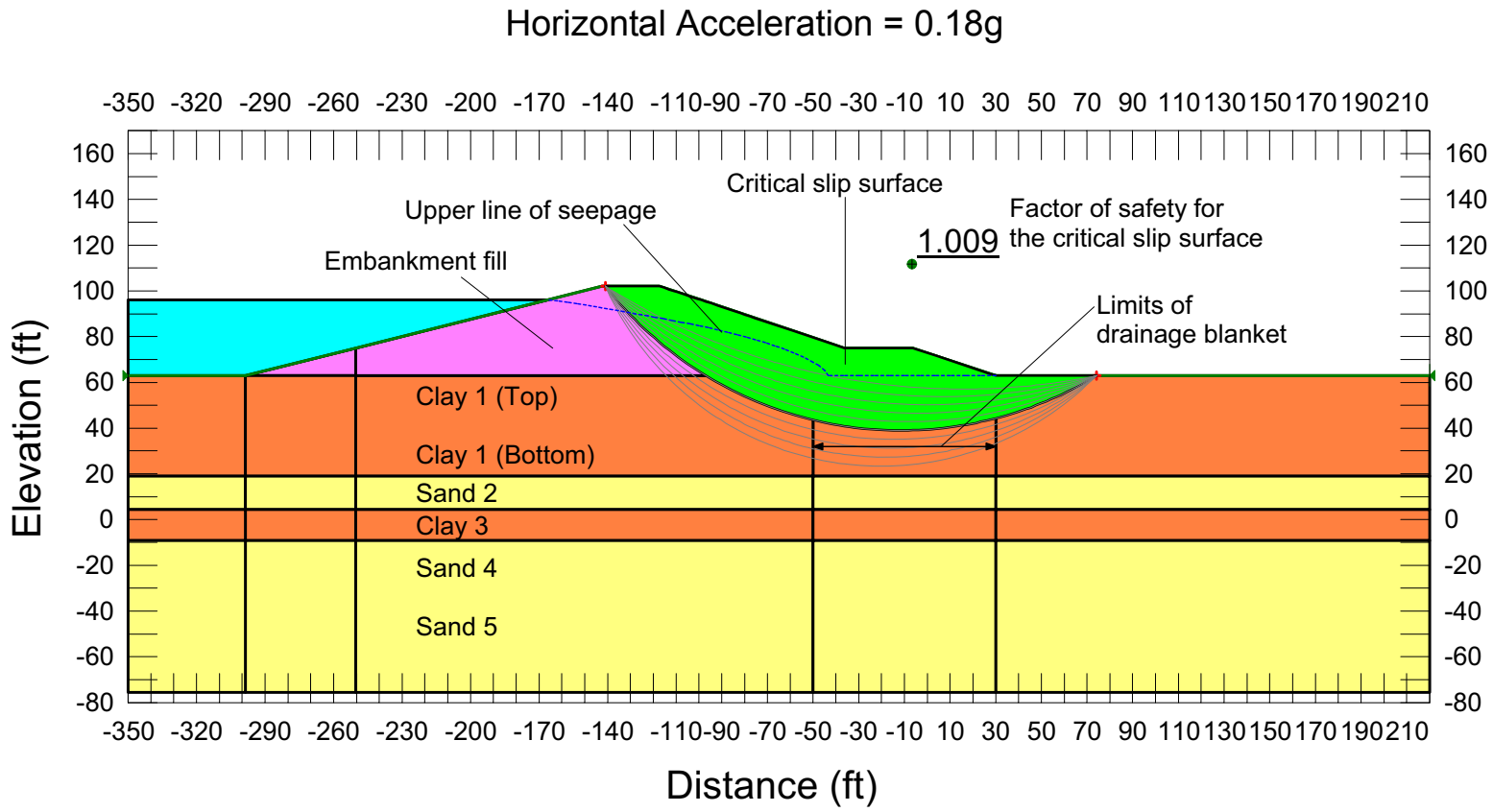

Notes:
Horizontal lines represent subsurface stratification and embankment fill limits
Vertical lines represent different region generation
Factor of safety is shown at a convenient location on the figure; does not represent the actual center point of the slip circle

Figure 2.5.5-230 Slope Stability; Yield Acceleration; South Dam of Cooling Basin at Boring B-2352

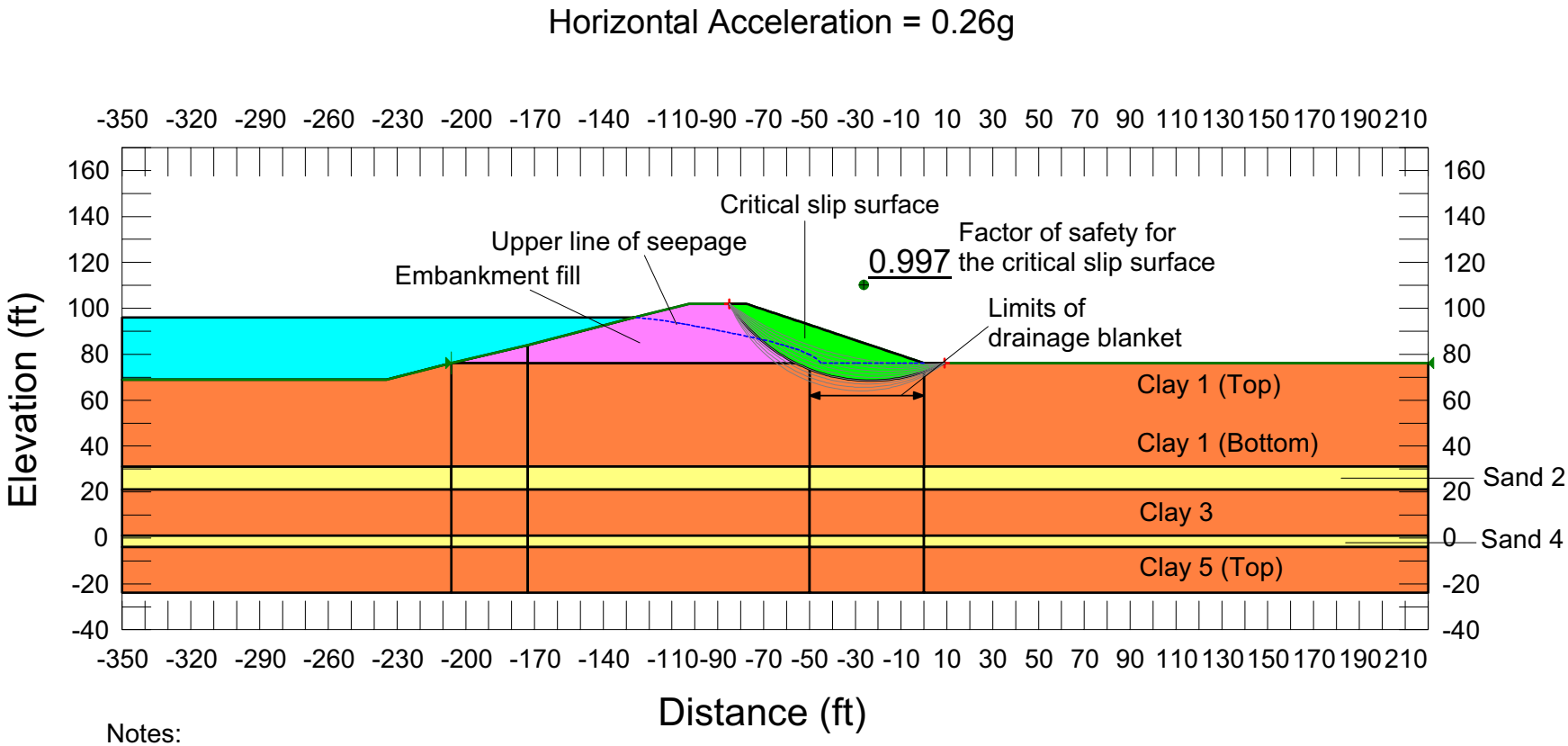

Notes:
Horizontal lines represent subsurface stratification and embankment fill limits
Vertical lines represent different region generation
Factor of safety is shown at a convenient location on the figure; does not represent the actual center point of the slip circle

Figure 2.5.5-231 Slope Stability; Yield Acceleration; West Dam of Cooling Basin at Boring B-2333

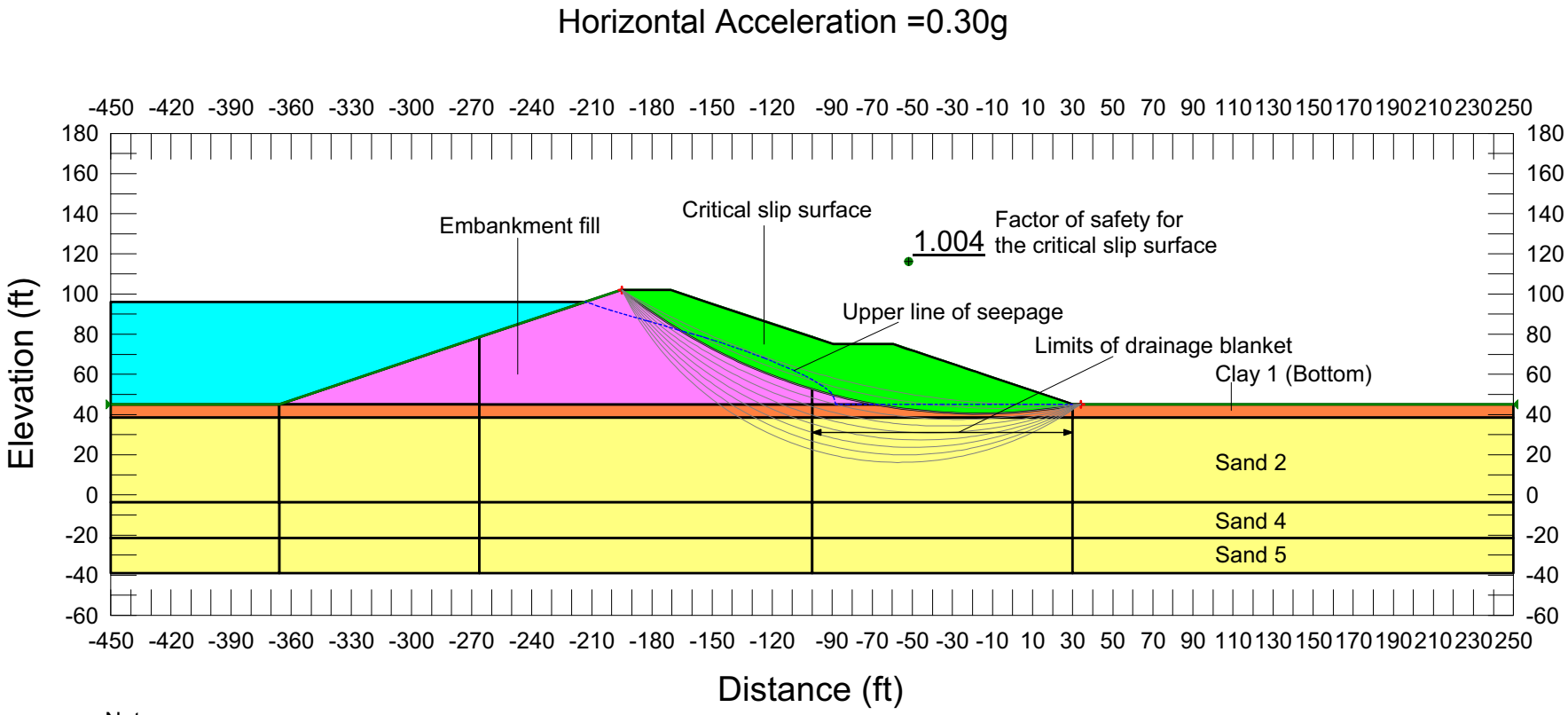

Notes:
Horizontal lines represent subsurface stratification and embankment fill limits
Vertical lines represent different region generation
Factor of safety is shown at a convenient location on the figure; does not represent the actual center point of the slip circle

Figure 2.5.5-232 Slope Stability; Yield Acceleration; East Dam of GBRA Storage Water Reservoir at Cone Penetration Test C-2317

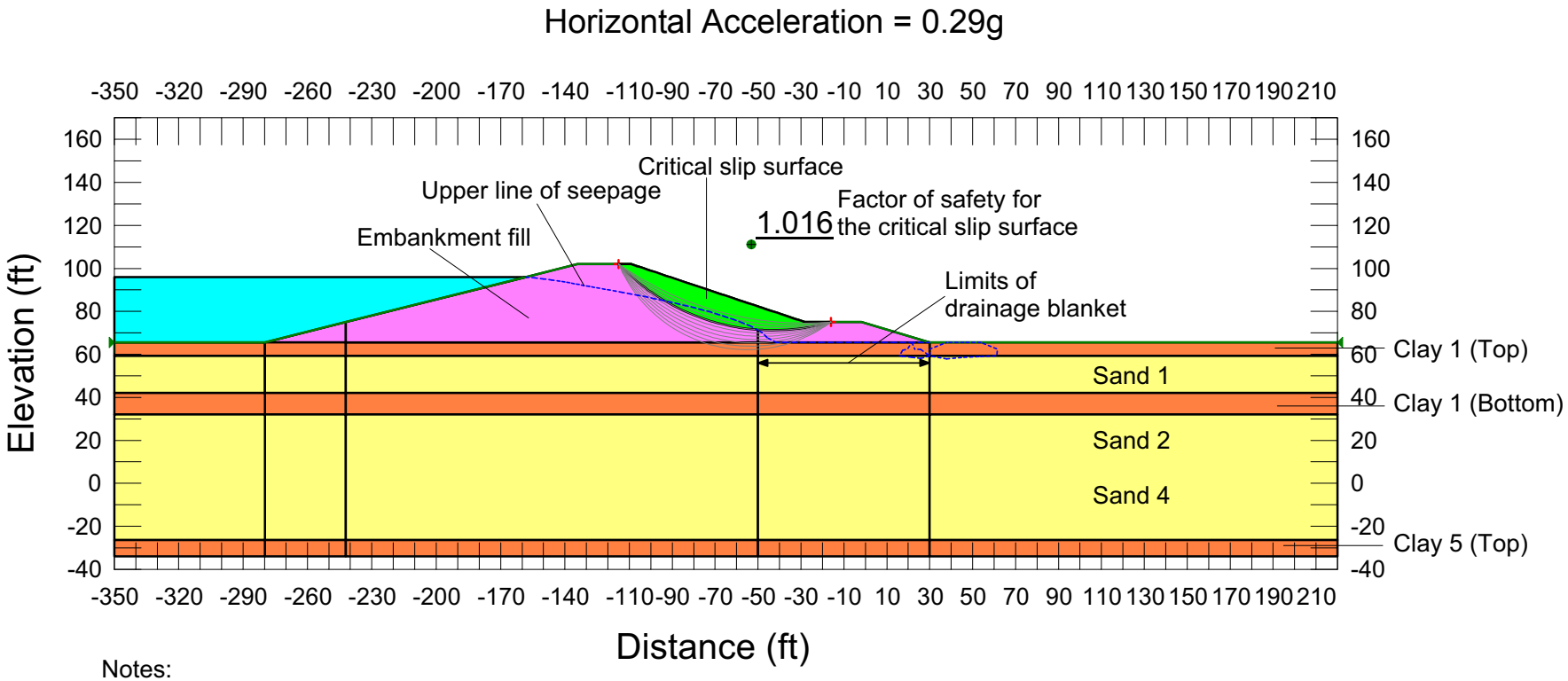

Notes:
Horizontal lines represent subsurface stratification and embankment fill limits
Vertical lines represent different region generation
Factor of safety is shown at a convenient location on the figure; does not represent the actual center point of the slip circle

**Figure 2.5.5-233 Slope Stability; Yield Acceleration;
East Dam of GBRA Storage Water Reservoir at Boring B-2353**

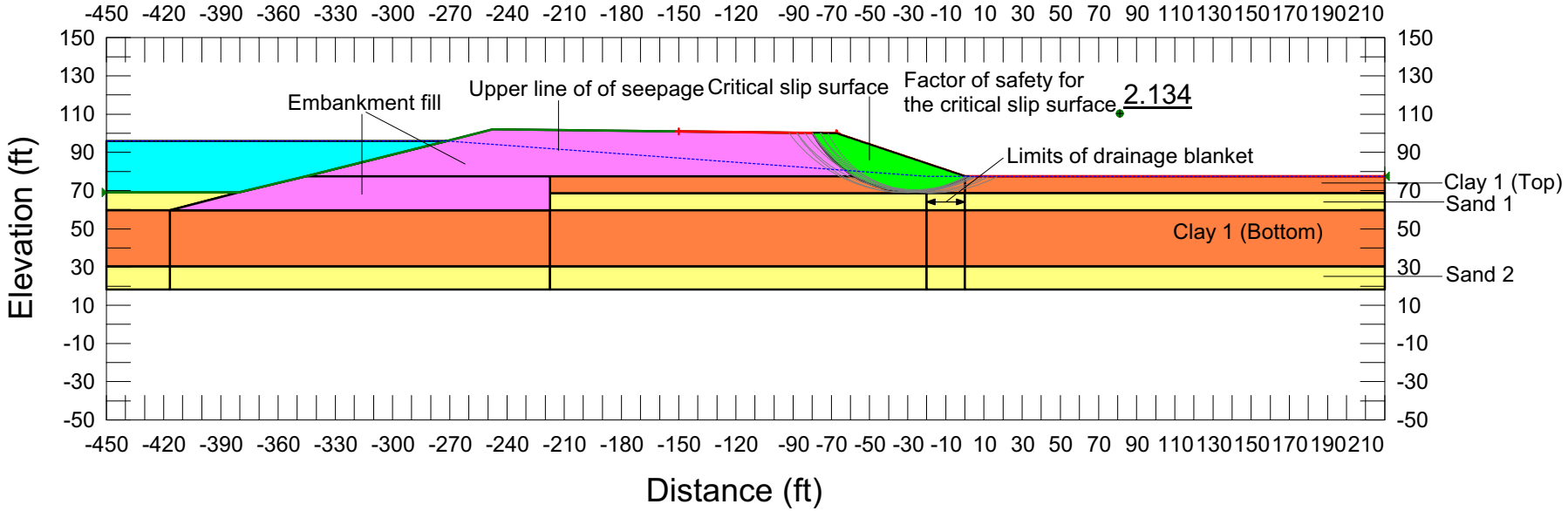

Notes:
Horizontal lines represent subsurface stratification and embankment fill limits
Vertical lines represent different region generation
Factor of safety is shown at a convenient location on the figure; does not represent the actual center point of the slip circle

Figure 2.5.5-234 Slope Stability; Post-Earthquake Case; North Dam of Cooling Basin at Cone Penetration Test C-2302

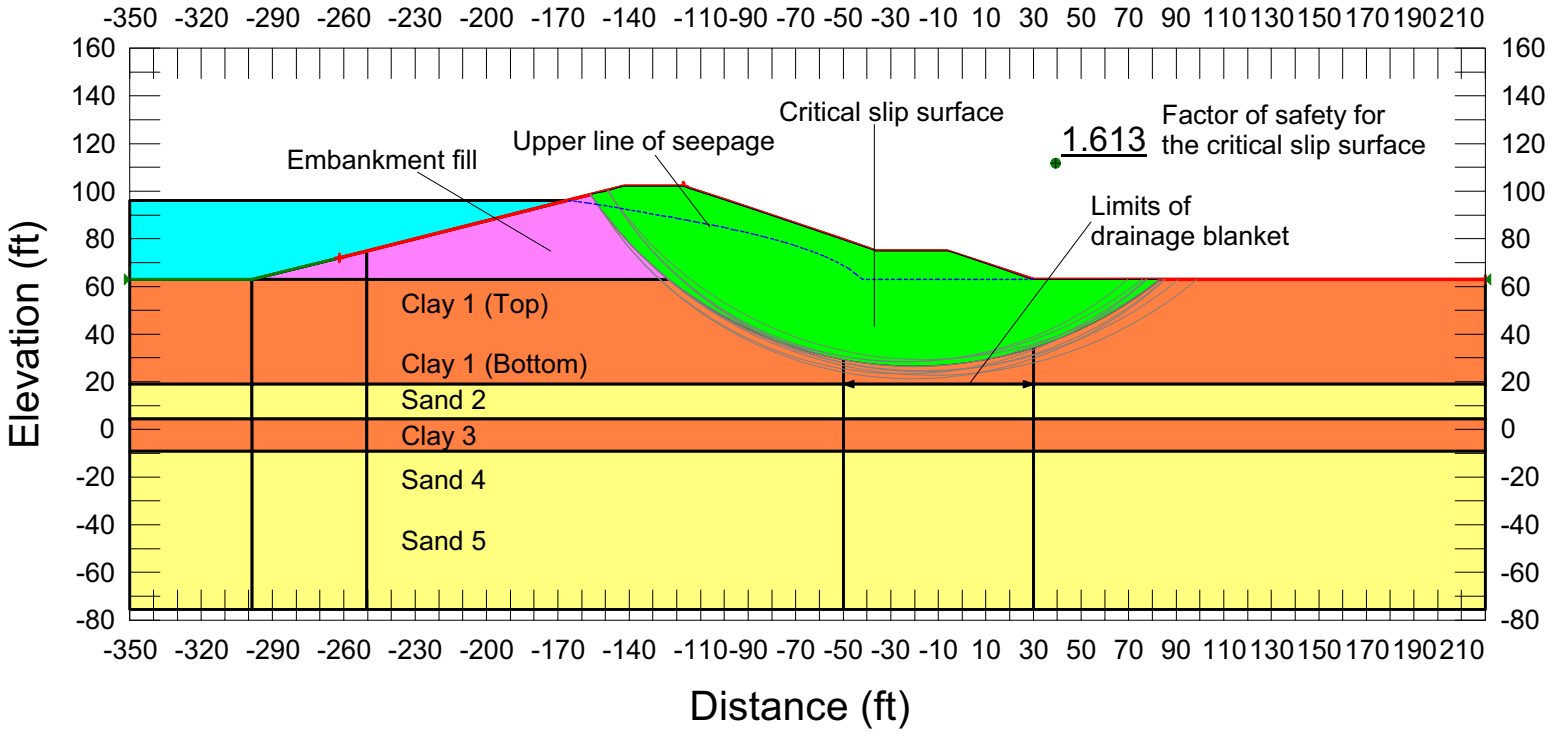

Notes:
Horizontal lines represent subsurface stratification and embankment fill limits
Vertical lines represent different region generation
Factor of safety is shown at a convenient location on the figure; does not represent the actual center point of the slip circle

Figure 2.5.5-235 Slope Stability; Post-Earthquake Case; South Dam of Cooling Basin at Boring B-2352

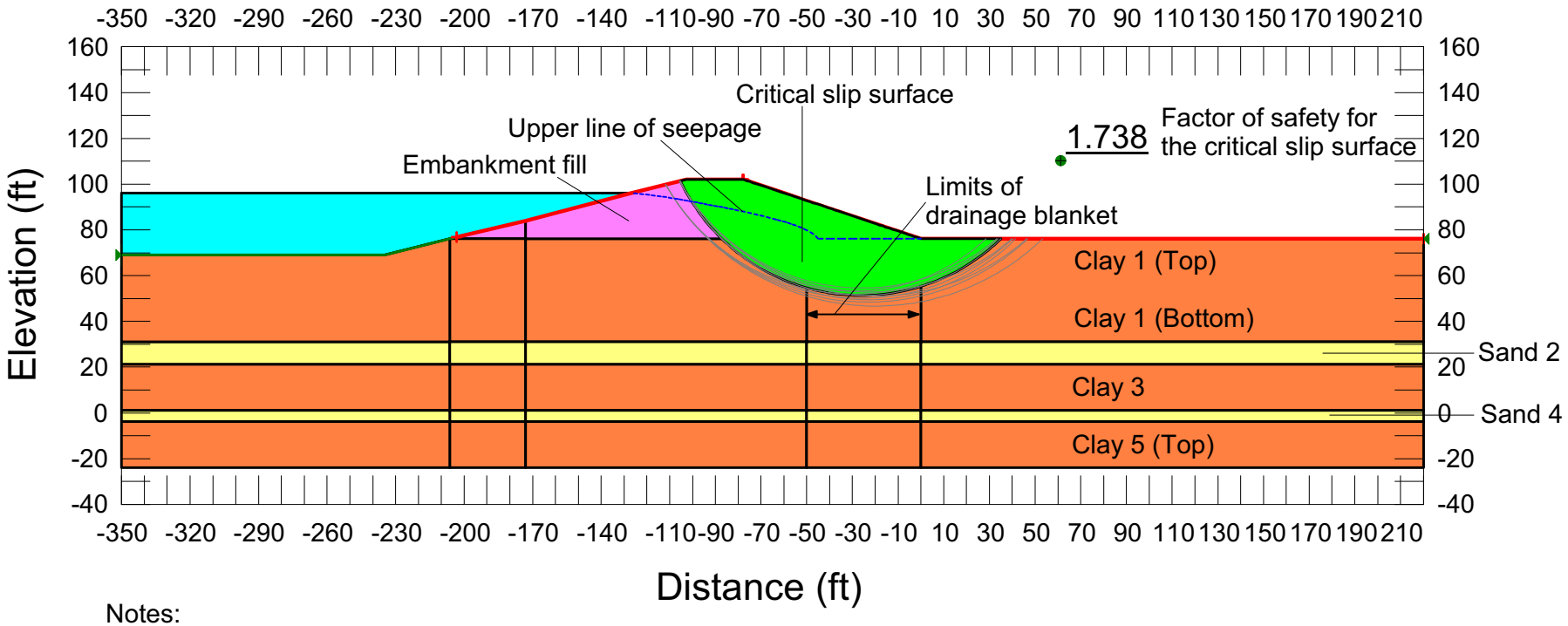

Notes:
Horizontal lines represent subsurface stratification and embankment fill limits
Vertical lines represent different region generation
Factor of safety is shown at a convenient location on the figure; does not represent the actual center point of the slip circle

Figure 2.5.5-236 Slope Stability; Post-Earthquake Case; West Dam of Cooling Basin at Boring B-2333

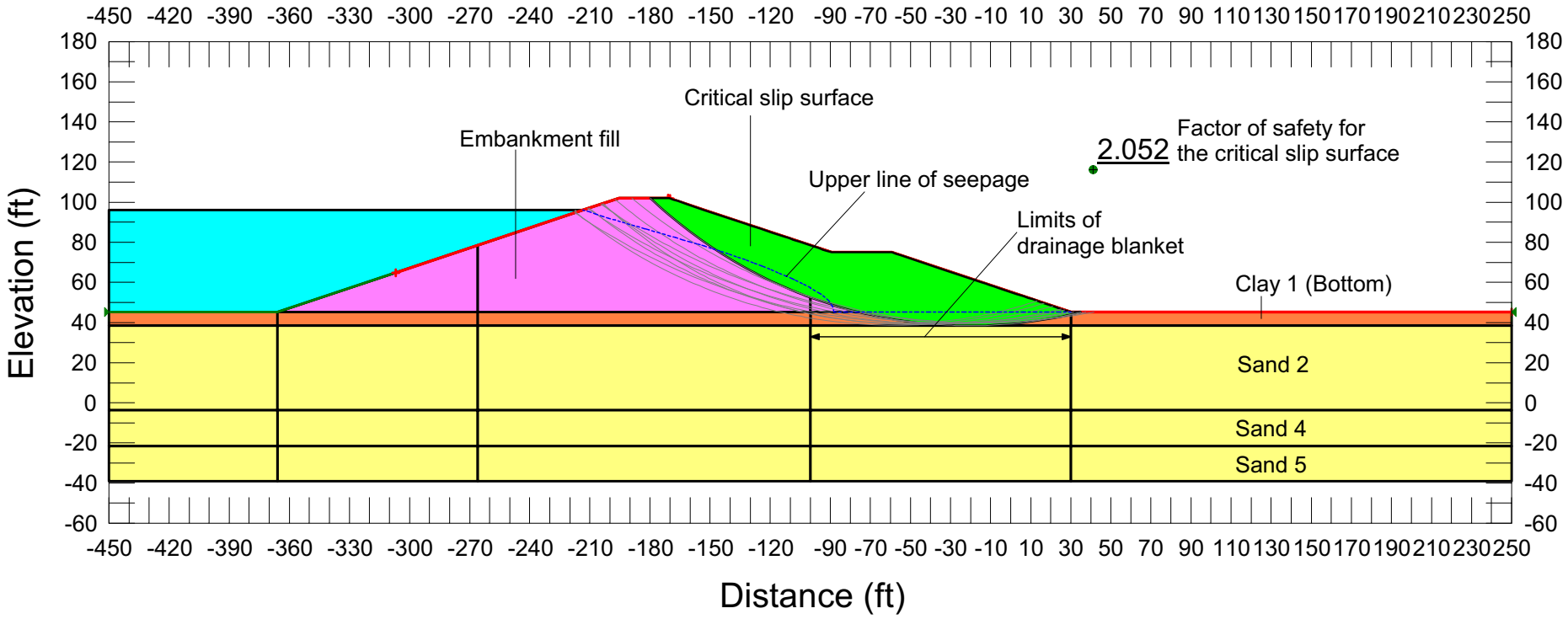

Notes:
Horizontal lines represent subsurface stratification and embankment fill limits
Vertical lines represent different region generation
Factor of safety is shown at a convenient location on the figure; does not represent the actual center point of the slip circle

**Figure 2.5.5-237 Slope Stability; Post-Earthquake Case;
East Dam of GBRA Storage Water Reservoir at Cone Penetration Test C-2317**

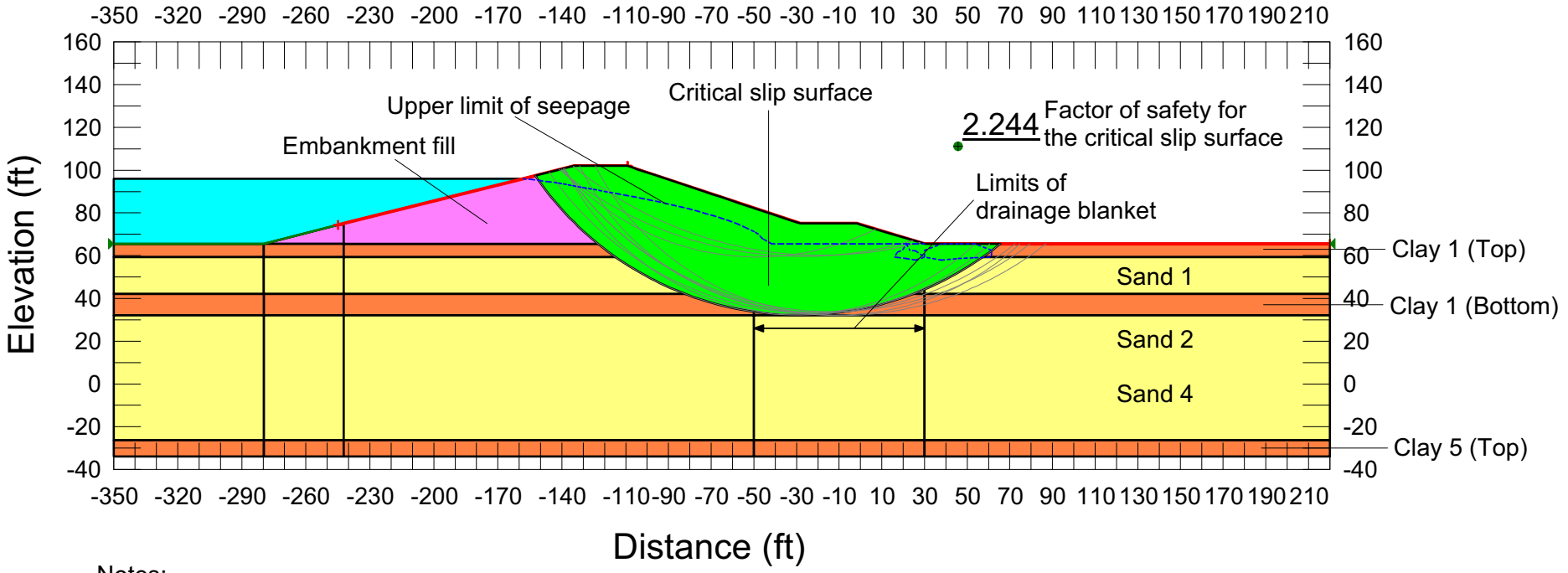

Notes:
Horizontal lines represent subsurface stratification and embankment fill limits
Vertical lines represent different region generation
Factor of safety is shown at a convenient location on the figure; does not represent the actual center point of the slip circle

Figure 2.5.5-238 Slope Stability; Post-Earthquake Case; East Dam of GBRA Storage Water Reservoir at Boring B-2353

Appendix 2.5.5-AA

Computer Software SLOPE/W and SEEP/W v.6.13 (Geo-Slope International, Ltd)

(2 pages)

2.5.5-AA Computer software SLOPE/W and SEEP/W v.6.13 (Geo-Slope International, Ltd.)

The abstract presented here is based on the information obtained from References 2.5.4-220 and 2.5.4-221.

The initial code for SLOPE/W was developed by Prof. D.G. Fredlund at the University of Saskatchewan. In the 1980s, the code was rewritten for the PC environment and named PC-SLOPE/W. Later, a graphical user interface was added to reflect the Microsoft Windows environment and the software was renamed as SLOPE/W.

SLOPE/W uses the theory of limit equilibrium of forces and moments to compute the factor of safety against failure. Using limit equilibrium, SLOPE/W can model complex stratigraphic and slip surface geometries, as well as variable pore water pressure conditions, using various soil models.

The factor of safety computed by SLOPE/W is defined as a factor by which the shear strength of the soil must be reduced to bring the mass of soil into a state of limiting equilibrium along a selected slip surface. The stability analysis involves passing a slip surface through the earth mass and dividing the inscribed portion into vertical slices. The slip may be circular or composite (i.e., circular and linear), or it may consist of any shape defined by a series of straight lines. The limit equilibrium formulation assumes that (1) the factor of safety of the cohesive component of strength and the frictional component of strength are equal for all soils involved, and (2) the factor of safety is the same for all slices. In slope stability analysis, SLOPE/W can use the methods of Ordinary, Janbu's simplified, Bishop's simplified, GLE, and Morgenstern-Price. Material properties may be defined by the soil models of Mohr-Coulomb, Bilinear, strength as a function of depth, and strength as a function of overburden pressure. Pore water pressures can be generated using Ru coefficients, piezometric lines, and finite-element computed total heads or pressures. The potential slip surfaces can be defined by a grid of centers and radius lines, entry and exit ranges, and blocks of slip surface points.

Once the stability problem is solved, SLOPE/W offers tools for viewing the results. It displays the slip surfaces and the corresponding factors of safety. Information about the critical slip surfaces, including the total

sliding mass and a force polygon showing the forces acting on each slice, can be obtained.

SEEP/W is a finite element software used for analyzing groundwater seepage and excess pore water pressure dissipation problems within porous materials under saturated steady-state problems or saturated/unsaturated time-dependent problems. Using the pore water pressures computed in SLOPE/W, it is possible to analyze saturated/unsaturated conditions for slope stability analysis.

Broadly speaking, there are three main parts involved in performing a SEEP/W analysis. The first is meshing, the process of subdividing the domain into small areas called finite elements. The second part is specifying and assigning material properties. The third is specifying and applying boundary conditions. SEEP/W is formulated for conditions of constant total stress, meaning that there is no loading or unloading of the soil mass. It uses Gaussian numerical integration to evaluate the element characteristic matrix and the mass matrix.

Once the seepage problem is solved, SEEP/W offers tools for viewing the results. As some of the features, it displays the contours of total heads, pressures, and gradients.